The homeoprotein ENGRAILED-1 promotes motoneuron survival and motor functions

Abbreviated title: **Motoneuron protection by ENGRAILED-1**

Stephanie E. Vargas Abonce[1,2], Mélanie Lebœuf[1,2], Kenneth L. Moya[1] and Alain Prochiantz[1,2,3]

[1]Centre for Interdisciplinary Research in Biology (CIRB), Collège de France, CNRS UMR 7241 / INSERM U1050, PSL Research University, Labex Memolife Paris Science et Lettres, 11 place Marcelin Berthelot 75005 Paris
[2]BrainEver, 74 rue du Faubourg Saint Antoine, 75012 Paris
[3]Institute of Neurosciences, Chinese Academy of Sciences, 320 Yueyang Rd, Shanghai 200031, China

Author contributions: SEVA and ML contributed equally to this paper. AP and KLM designed research; SEVA and ML performed research; SEVA, ML and KLM analyzed data, SEVA, ML, AP and KLM wrote the paper.
Correspondence to ken.moya@college-de-france.fr or alain.prochiantz@college-de-france.fr

Acknowledgements: We thank the College de France imaging and animal facilities. We thank Dr. Anne-Cécile Boulay for assisting us in RNAscope experiments, Drs. Anne Bousseau and Yoko Arai for helpful discussions and Angélique Bibimbou for excellent technical assistance.

Conflict of Interest Statement: AP and KLM are listed on several patents for the use of HPs for the treatment of neurodegenerative disease. They are co-founders and hold shares in a company developing HPs for therapeutic use. SEVA and ML are BrainEver post-doctorant and doctorant, respectively.

Funding sources: MemoLife Labex PhD fellowship to SEVA, Association Nationale de la Recherche et de la Technologie (Cifre/ANRT n° 2017/0488) to ML, BrainEver, HomeoSign ERC -2013-AdG n°339379.

ABSTRACT

In addition to their cell-autonomous activities, a number of homeoprotein transcription factors transfer between cells and regulate gene transcription, protein translation and chromatin organization in a non-cell autonomous way. ENGRAILED-1 homeoprotein has the latter properties and is expressed in spinal cord V1 interneurons that synapse on large α-motoneurons. Because several homeoproteins have neuroprotective effects in the central nervous system, we analyzed the motor phenotype of mice with reduced extracellular spinal cord ENGRAILED-1 or lacking one functional *Engrailed-1* allele. These mice show progressive muscle weakness, abnormal spinal reflex and partial neuromuscular junction denervation. In the *Engrailed-1* heterozygote, large α-motoneuron degeneration is first observed at 4.5 months of age and progresses to reach 50 per cent loss in 15.5-month-old mice. A single intrathecal injection of exogenous recombinant human ENGRAILED-1 at 3 months in the lumbar enlargement of the heterozygote results in the addressing of the protein to α-motoneurons. This fully restores endplate innervation, limb strength and extensor reflex for at least 3 months, and prevents the death of lumbar α-motoneurons. Bioinformatic analysis identified the autophagy gene *p62* as an *Engrailed-1* target in spinal cord α-motoneurons and demonstrated both its upregulation in the heterozygote and its return to normal expression levels following ENGRAILED-1 injection. These results identify a direct non-cell autonomous activity of ENGRAILED-1 in spinal cord α-motoneuron survival and function and demonstrate that a single injection of the transcription factor in the *Engrailed-1* heterozygote prevents α-motoneuron degeneration and strength loss for several months.

INTRODUCTION

First discovered on the basis of their developmental functions[1], homeoprotein (HP) transcription factors are also expressed in the adult, suggesting that they participate in physiological homeostasis[2]. As shown in several animal and plant models, HP functions involve both cell autonomous and non-cell autonomous activities[3]. Direct non-cell autonomous properties arise from the ability of HPs to transfer between cells due to two highly conserved sequences present in their DNA-binding domain[4,5]. Examples of *in vivo* non-cell autonomous activities in the central nervous system, include the regulation of cerebral cortex plasticity by OTX2[6,7] the control of oligodendrocyte precursor cell and Cajal-Retzius cell migration by PAX6[8] and the axon guidance activities of ENGRAILED and VAX-1[9,10].

An important ENGRAILED-1 (EN1) function is to maintain the survival of mesencephalic dopaminergic (mDA) neurons of the Substantia Nigra pars compacta (SNpc). In *Engrailed-1* heterozygote (*En1-Het*) mice, mDA neurons die progressively starting at post-natal week 6 with approximately 60% of them remaining in one-year-old mice[11]. Infusion or injection of EN1 or EN2 proteins in the SNpc, followed by their internalization by mDA neurons, rescues these neurons from degeneration in several Parkinson Disease (PD) mouse and non-human primate models[12–14]. A single EN1 injection in mice rescues mDA for several weeks, reflecting that EN1, in addition to directly regulating transcription and translation [15,16], also works as an epigenetic chromatin remodeler[13,17].

En1, but not *En2*, is expressed in developing and early postnatal ventral spinal cord V1 inhibitory interneurons, including Renshaw cells, that form inhibitory GABAergic and glycinergic synapses on large α-motoneurons (αMNs) and regulate alternating flexor-extensor activity[18,19]. With the excitatory V0 interneurons, the inhibitory V1 interneurons contribute to an excitatory/inhibitory balance that may be important for αMN survival[20].

In light of our studies demonstrating that EN1, EN2 and OTX2 have neuronal pro-survival activities[3], we investigated whether EN1 expressed by V1 interneurons may be important for αMN physiology and survival with which they are in synaptic contact. We demonstrate that *En1* expression is maintained in adulthood and that *En1-Het* mice have early muscle weakness

and abnormal spinal reflex associated with partial denervation of the neuromuscular junction (NMJ) and a later loss of αMNs. These deficits are progressive, increase after 2 to 3 months of age and are, in part, reproduced by blocking EN1 non-cell autonomous activity. Importantly, a single intrathecal injection of human recombinant EN1 (hEN1) at 3 months restores muscle strength, normalizes spinal reflex and NMJ innervation and promotes αMN survival. This restorative and protective activity lasts for at least 3 months.

MATERIALS AND METHODS

Animal Management

All animal treatments followed the guidelines for the care and use of laboratory animals (US National Institutes of Health), the European Directive number 86/609 (EEC Council for Animal Protection in Experimental Research and Other Scientific Utilization) and French authorizations n° 00703.01 "Therapeutic homeoproteins in Parkinson Disease" and n° APAFIS #6034-2016071110167703 v2, "Spinal cord motoneuron neuroprotection" delivered by the Minister of higher education, research and innovation. Adult mice were housed two to five per cage with *ad libitum* access to food and water and under a 12h light/dark cycle. Transgenic mouse strain *En1-Het* was bred by the Rodent Breeding Services provided by the Animal Care Services at College de France. Colony maintenance and genotyping were performed as previously described[21]. Females and males were included in all studies. The endpoint limit for euthanasia was a 15% or greater loss of bodyweight or signs of paralysis; in all experiments, no mouse reached these endpoints.

Behavioral analyses

We used forepaw grip strength, inverted grid and hindlimb extension reflex tests. Mice were habituated to the behavioral room and to the experimenter 24 hours before the day of testing and again 1 hour before each behavioral test. All tests were performed on the same day and behavioral assessment was carried by evaluators blind to genotype and treatment. Mice were weighed before each session.

Forepaw Grip Strength. The Transducer (IITC Life Science Grip Strength Meter, ALMEMO 2450 AHLBORN, World Precision Instruments) was calibrated and the scale of values set to grams. Each mouse was lifted by the tail to position the front paws at the height of the bar (about 15 cm) and then moved towards the bar. When symmetric firm grip with both paws was established the mouse was pulled backward at a constant speed until the grasp was broken and the maximal value was recorded. The test was repeated 5 times per animal with a minimal resting time of 5 minutes between tests and the mean of all values was normalized to the weight of each animal. At least 4 mice per group per experiment were used.

Inverted Grid Test. The mouse was placed on a wire grid (15x10 cm) and allowed to explore it. After 3-5 minutes, the grid was raised 30 cm above a soft surface and slowly inverted. Latency

to release was recorded three times per mouse with a minimum resting time of 5 minutes between trials. The longest latency was used for analysis.

Hindlimb Extensor Reflex. Mice were suspended by the tail at a constant height (30 cm) and scored for hindlimb extension reflex. The scores were assigned from 0 to 3 as follows: 3 for normal symmetric extension in both hind limbs without visible tremors; 2.5 for normal extension in both hind limbs with tremor in one or both paws; 2.0 for unequal extension of the hind limbs without visible tremors; 1.5 for unequal extension in the hind limbs with tremors in one or both paws, 1.0 for extension reflex in only one hindlimb, 0.5 for minimum extension of both hindlimbs, 0 for absence of any hindlimb extension.

Tissue preparation

Spinal cord. Adult mice were euthanized by a 1 µl/g body weight dose of Dolethal (Euthasol: 4 µg/µl). Spinal cords were dissected after laminectomy and placed in Phosphate Buffer Saline (PBS) to remove meninges and surrounding connective tissues. Cervical and lumbar enlargements were separately placed in paraformaldehyde 4% (PFA, Thermo Scientific) for 1 h at room temperature (RT) with gentle mixing, washed in PBS three times for 30 minutes at RT and placed in PBS with 20% sucrose overnight at 4°C. After cryoprotection, the tissue was embedded in Tissue Freezing Medium (TFM, Microm Microtech), frozen on dry ice and 30 µM sections prepared using an HM 560 Microm cryostat (Thermo Scientific).

Muscle. The extraocular muscle (EOM), tongue and lumbrical muscles from the plantar surface of the paw were dissected in cold PBS and fixed at RT in 4% PFA for 10 minutes for extraocular and lumbrical muscles (1 hour for the tongue) washed in PBS and cryoprotected. Extraocular and lumbrical muscle whole-mounts were processed *in toto* to visualize the entire innervation pattern and detailed analysis of the neuromuscular junctions[22]Tongue muscles were embedded and sectioned at 30 µm.

Cresyl violet staining. Slides with 30 µm spinal cord sections were washed in PBS 3 times, cleared in O-Xylene (CARLO-HERBA) for 5 minutes, then hydrated in graded alcohols with increasing water and placed in Cresyl Violet acetate (MERCK). Sections where then dehydrated in increasing alcohol and mounted in Eukitt® Quick-hardening mounting medium (Sigma).

Spinal cord and muscle immunofluorescence labeling. Slides with 30 µm spinal cord or muscle sections were washed in PBS and permeabilized with 2% Triton. After 30 minutes at RT in 100 µM glycine buffer, sections were blocked in 10% Normal Goat Serum (NGS, Invitrogen) or Fetal Bovine Serum (FBS, Gibco) in the presence of 1% Triton and incubated with primary antibodies (sheep anti-Choline Acetyltransferase (ChAT) ABCAM 1:1000, goat anti-ChAT Millipore 1:500, rabbit anti-EN1 1:300[11], mouse anti-neurofilament 165kDa DSHB 1:50, mouse anti-synaptic vesicle glycoprotein 2A DSHB 1:100 and rabbit anti-p62 ABCAM 1:1000) overnight at 4°C, washed and further incubated with secondary antibodies for 2 hours at RT. For muscle staining, α-bungarotoxin (Alexa Fluor 488 conjugate) was included at the same time as the secondary antibodies. Slides were washed and mounted with DAPI Fluoromount-G® (Southern Biotech). Controls without primary antibodies were systematically included.

RT-qPCR

Spinal cords were removed as above and lumbar enlargements were rapidly frozen on dry ice. Total RNA was extracted (RNeasy Mini kit, Qiagen) and reverse transcribed using the QuantiTect Reverse Transcription kit (Qiagen). RT-qPCR was done using SYBR-Green (Roche Applied Science) and a Light Cycler 480 (Roche Applied Science). Data were analyzed using the "2-ddCt" method and values were normalized to *Glyceraldehyde 3-phosphate dehydrogenase* (*Gapdh*). The following primers were used: *Engrailed-1* sense: CCTGGGTCTACTGCACACG, antisense: CGCTTGTTTTGGAACCAGAT; *Gapdh* sense: TGACGTGCCGCCTGGAGAAAC, antisense: CCGGCATCGAAGGTGGAAGAG.

Protein production

Human EN1 (hEN1) was produced as described[23] and endotoxins were removed by Triton X-144 phase separation. In brief, pre-condensed 1% Triton X-144 (Sigma) was added to the protein preparation. The solution was incubated for 30 minutes at 4°C with constant stirring, transferred to 37°C for 10 minutes and centrifuged at 4000 rpm for 10 minutes at 25°C. The endotoxin-free protein was aliquoted and kept at -80°C.

Intrathecal injections

Mice were anesthetized with 1 µl/g ketamine-xylazine (Imalgene1000: 10 µg/µl, Ruompur 2%: 0,8 µg/µl) and placed on the injection platform. The tail of the animal was taken between two fingers and the spinal column was gently flattened against a padded surface with the other hand.

The L3 vertebral spine was identified by palpation and a 23G x 1" needle (0.6x25 mm Terumo tip) was placed at the L1 and T13 groove and inserted through the skin at an angle of 20°[24].The needle was slowly advanced into the intervertebral space until it reached the injection point, provoking a strong tail-flick reflex. Five µl were injected at a rate of 1 µl/min with or without 1µg recombinant protein. The needle was left in place for two minutes after injection and then slowly removed. Animals were placed in a warmed chamber until recovery from anesthesia. Extensor reflex and gait analysis were examined 2 and 24 hours after injection to verify the absence of spinal cord damage.

RNAscope Fluorescent in Situ Hybridization

Mice aged 4.5 months were euthanized with Dolethal and transcardially perfused with 0.9% NaCl. The lumbar region of the spinal cord was dissected, fixed overnight in 4% PFA at 4°C and cryoprotected in PBS 30% sucrose for 48 hours at 4°C. Spinal cord sections 40 µm-thick were prepared using a Leitz (1400) sliding microtome. Sections were washed in PBS, incubated with RNAscope hydrogen peroxide solution from Advanced Cell Diagnostics (ACD) for 10 min at RT, rinsed in Tris-buffered saline with Tween (50 mM Tris-Cl, pH 7.6; 150 mM NaCl, 0.1% Tween 20) at RT, collected on Super Frost plus microscope slides (Thermo Scientific), dried at RT for 1 hour, rapidly immersed in ultrapure water, dried again at RT for 1 hour, heated for 1 hour at 60°C and dried at RT overnight. The next day, sections were immersed in ultrapure water, rapidly dehydrated with 100% ethanol, incubated at 100°C for 15 minutes in RNAscope 1X Target Retrieval Reagent (ACD), washed in ultrapure water and dehydrated with 100% ethanol for 3 minutes at RT. Protease treatment was carried out using RNAscope Protease Plus solution (ACD) for 30 minutes at 40°C in a HybEZ oven (ACD). Sections were then washed in PBS before *in situ* hybridization using the RNAscope Multiplex Fluorescent V2 Assay (ACD). Probes were hybridized for 2 hours at 40°C in HybEZ oven (ACD), followed by incubation with signal amplification reagents according to the manufacturer's instructions. Probes were purchased from ACD: Mm-*En1*-C1 (catalog #442651), Mm-*Chat*-C2 (catalog #408731-C2), Mm-*Calb1*-C3 (catalog #428431-C3). The hybridized probe signal was visualized and captured on an upright Leica CFS SP5 confocal microscope with a 40x oil objective.

Bioinformatic analysis

Differentially expressed genes (cutoff $p<0.05$) from the RNA-seq performed on microdissected six-week-old SNpc from wild type (WT) and *En1-Het* mice (GSE72321[13]) were compared to genes identified from an RNAseq of microdissected MNs from WT mice (GSE38820[25]).

Transcripts present in the two lists were retained. Using STRING database, 10 biological processes of interest were selected including regulation of gene expression, cellular response to stress, cell communication, regulation of I-kappaB kinase/NF-kappaB signaling, cellular response to DNA damage stimulus, response to oxygen-containing compounds, locomotion, DNA repair, modulation of chemical synaptic transmission, and brain development. Using these pathways reduced the list of selected genes to 402. The interaction of the selected genes with the four main genes involved in familial ALS (fALS): *Sod1*, *Fus, C9Orf72* and *Tardbp* was investigated.

Image analyses

Cresyl violet stained spinal cord section images were acquired with a Nikon-i90 microscope under bright field conditions at 10x with a Z-stack step of 0.5 µm. Immunofluorescence stained spinal cord sections images were acquired with a Leica SP5 inverted confocal microscope at 20x (Leica DMI6000) and acquisitions of 3D z-stack (0.5 µm) were made using the UV (405 nm, 50 mW), Argon (488 nm, 200 mW) and DPSS (561 nm, 15 mW) lasers. For cell quantification, at least five spinal cord sections separated by $\geq$ 900 µm were analyzed for each animal. ChAT+ cells and Cresyl violet stained cells with a soma area above 100 μm^2 were manually outlined using ImageJ software (NIH, Bethesda, MD) and their area determined. Analyses were carried out on Z-stacks through the entire 30 µm thickness of the section. Cells were classified as small (100-199 μm^2 cross sectional area), intermediate (200-299 μm^2) or large (> 300 μm^2). Supplemental Figure 1 illustrates that ChAT and Cresyl violet gave similar results for medium size (200-299 μm^2) and large (>300 μm^2) neurons thus allowing us to characterize αMNs on the basis of size (>300 μm^2), with or without additional ChAT staining. For p62 staining analysis, the motoneuron region of five lumbar sections were acquired at 40x for each animal. The mean intensity was measured in ChAT+ cells with a soma greater than 300 μm^2 using ImageJ software. For each experiment, image acquisition was performed with the same parameter settings of the confocal microscope to allow for comparison between experimental conditions.

Lumbrical, EOM and tongue muscles were imaged with a Leica SP5 inverted confocal microscope (Leica DMI6000) with a motorized XY stage. 3D z-stack (0.5 µm) acquisitions were made as above (UV, Argon and DPSS) and images analyzed using ImageJ software. Analyses were performed blind to the genotype and treatment. Endplates where categorized as fully innervated (neurofilament overlying more than 80% of the endplate), partially innervated

(neurofilament overlying up to 80% of the endplate) or denervated (no neurofilament overlying the endplate)[26]. Endplate morphology was evaluated by counting the number of endplates with perforations (areas lacking α-bungarotoxin staining). For postsynaptic analysis, each endplate was manually outlined using ImageJ software and its area calculated. All analyses were performed on the entire Z-stacks through the NMJ.

Statistical analyses

Results are expressed as mean ± SD. Statistical significance was determined as follows. For RT-qPCR, WT and *En1-Het* mice were compared by Unpaired T-test with equal SD. For behavioral and NMJ analyses and αMN counting in the time-course study, groups were compared by Unpaired T-test with equal SD comparing WT with *En1-Het* for each time point. For intrathecal injections, behavioral and NMJ analyses and αMN counting, experimental data were compared by one-way ANOVA followed by a post hoc Dunnett's test for comparisons to WT. For behavioral analysis in the time-course protection of injected hEN1, groups were compared by Unpaired T-test with equal variances comparing WT with *En1-Het* injected at each time point.

RESULTS

Engrailed-1 is expressed in the adult spinal cord and neutralizing extracellular EN1 induces motor deficits

Previous studies reported *En1* expression in V1 interneurons in the early postnatal mouse spinal cord[27]. Figure 1a shows that this expression is maintained at 4.5 months in a large population of neurons located dorsally to the main population of large ChAT-stained MNs and in the ventral Calbindin-1 positive Renshaw cells. The selectivity of the probe for EN1 is demonstrated in Supplemental Figure 2a by the hybridization in the Ventral Tegmental Area and Substantia Nigra, two midbrain structures that contain an important population of *En1*-expressing mesencephalic dopaminergic neurons[28]. Figure 1b compares the expression of *En1* by RT-qPCR at 4.5 and 16 months in the spinal cord of WT and *En1-Het* mice. This expression is reduced by twofold, as expected, in the *En1* heterozygote and, for each genotype, does not decrease between the two ages analyzed. Supplemental Figure 2b suggests that this reduction affects the entire *En1*-expressing domain in the spinal cord. This first series of experiments allows us to conclude that the large ChAT-expressing MNs are surrounded by a population of *En1*-expressing cells.

We previously demonstrated that similarly to several HPs, EN1/2 is a transduction protein that directly signals between cells[3,29]. Neutralizing EN1/2 *in vivo* in the extracellular space modifies the maturation of the anterior cross vein in the fly wing disk[30] and permits the growth of temporal retinal ganglion cell growth cones into the Xenopus and chick posterior tectum[9]. In the latter example, neutralization of extracellular EN1/2 was achieved by the *in vivo* expression of a secreted single-chain antibody (scFv) directed against EN1/2. Here we examined whether neutralizing extracellular EN1 in the spinal cord with the same scFv antibody affects motor behavior. An AAV8 encoding the myc-tagged anti-EN1/2 under the control of the astrocyte-specific Glial Fibrillary Acidic Protein (GFAP) promoter was injected intrathecally at the lumbar level in 1-month-old WT mice (Fig. 2a).

We followed the effects of extracellular EN1 neutralization on weight and performed 3 tests evaluating muscular strength and a spinal reflex (Fig. 2b). Compared to a GFAP promoter driven mCherry-expressing AAV8 (control vector), the anti-EN1/2 scFv had an effect on weight, forepaw grip strength (grasping), the ability of the 4 limbs to resist gravity (inverted

grid) and the hind limb extensor reflex that measures purely spinal functions. The effect on weight appeared only 15 weeks after injection, whereas muscle weakness and abnormal hindlimb reflex appeared much earlier (Fig. 2b). In all cases, performance deteriorated with time. To understand the biological basis of the deficits, αMNs identified by size and ChAT expression (Supplemental Fig. 1) were counted 16 weeks following injection and Figure 2d shows that neutralizing extracellular EN1 for 16 weeks has no effect on their number. Alpha-bungarotoxin and antibodies against neurofilament and synaptic vesicle protein 2A were used to visualize acetylcholine receptor (AChR) clusters of the motor endplate and motor axon terminals, respectively. The percentage of fully innervated motor endplates was reduced 16 weeks following scFv injection (Fig. 2c). Thus, neutralizing extracellular EN1 results in a partial denervation of the neuromuscular junction.

Phenotypic characterization of the *En1-Het* mutant mouse

Given that EN1 is expressed in the adult spinal cord and that neutralizing it in the extracellular space has a deleterious effect on strength and motor end plate innervation, we examined the "motor" phenotype of the *En1-Het* mouse in which *En1* expression is reduced twofold (Fig. 1b). *En1-Het* mice display the same average weight gain as their WT littermates at all ages studied (Fig. 3a). For the three tests used to assess strength, WT and *En1-Het* animals evolved differently, the latter showing signs of loss of strength compared to their WT littermates (Fig. 3b-d). At 1 and 2 months of age, forepaw grip strength was similar in *En1-Het* and WT mice, but a significant reduction was first measured at 3 months that persisted through 15.5 months of age (Fig. 3b). In the inverted grid test, 2-month-old *En1-Het* mice held on significantly less time than WT mice; holding time further diminished between 2 and 3 months and remained reduced through 15.5 months (Fig. 3c). Finally, the hind limb extensor reflex was used to evaluate local lower spinal function. WT mice had a normal extensor score of about three at all ages but the score of the *En1-Het* animals deteriorated between 1 and 9 months (Fig. 3d). Taken together, these results show that compared to WT littermates, *En1-Het* mice show a rapid period of loss of strength between 1 and 4.5 months followed by a slower or stabilized degradation.

We analyzed NMJ morphology and synaptic characteristics of three muscle groups with different degrees of vulnerability in motoneuron diseases[26]. Data corresponding to lumbrical endplates are described in Figure 4 and those corresponding to extraocular and tongue muscles in Supplemental Figure 3. The typical endplate morphology well-centered on the lumbrical muscle fibers was observed in all mice examined (Fig. 4a)[22]. No changes were found in the

average number of AChR clusters between WT and *En1-Het* mice (Fig. 4b). The area of the motor endplate does not differ between WT and *En1-Het* mice through 9 months of age, but is significantly reduced in *En1-Het* mice at 15.5 months (Fig. 4c). Endplate perforations (post-junctional folds) are regions of the endplate devoid of AChR. Their number reflects the state of maturation of the NMJ and normal healthy muscles show a complex morphology with multiple perforations[31,32]. The percentage of endplates with perforations does not differ between WT and *En1-Het* mice through 9 months of age but is significantly reduced in the *En1-Het* mice at 15.5 months (Fig. 4d). Finally, the percentage of fully innervated motor endplates (neurofilament immunoreactivity overlaying more than 80% of the endplate) is significantly reduced in the *En1-Het* mice NMJ, starting at 3 months, worsening at 4.5 months and remaining reduced thereafter (Fig. 4e). In contrast with lumbrical endplates, no differences between the two genotypes were observed in any of the NMJ morphological characteristics for extraocular and tongue muscles, at any age (Supplemental Fig. 3).

We then analyzed the number of neurons present in the cervical and lumbar enlargements of the spinal cord in the *En1-Het* mice and their WT littermates. Visually, the total number of Cresyl violet-stained neurons in the ventral spinal cord cervical and lumbar enlargements appeared similar in WT and *En1-Het* mice at 15.5 months. In contrast, a decrease in the number of large densely stained cells was clearly apparent in the *En1-Het* mouse spinal cord (Fig. 5a). To understand this better, neurons were classified according to their surface: small neurons of 100-199 μm^2, intermediate size neurons of 200-299 μm^2, and large neurons > 300 μm^2. The number of small and intermediate sized neurons remained constant at all ages, with no difference between *En1-Het* and WT mice (Fig. 5b,c) while the number of large neurons decreased progressively between months 4.5 (≈ 20% loss) and 15.5 (≈ 50% loss) in the cervical and lumbar enlargements of *En1-Het* animals (Fig. 5d,e).

ChAT is selectively expressed in γ and αMNs which can be distinguished on the basis of size[32]. In order to better identify the neurons that are lost in the ventral spinal cord of *En1-Het* animals we analyzed ChAT immunoreactivity in 9-month-old mice. Compared to WT, *En1-Het* spinal cord clearly shows a loss of large > 300 μm^2 ChAT+ cells (Supplemental Fig. 1). Comparing Cresyl violet and ChAT staining for medium and large sized neurons confirmed that the cells that disappear in the *En1-Het* mutant are αMNs. It is of note that the partial loss of large αMNs in the *En1-Het* mouse spinal cord is not accompanied by a corresponding increase in the

intermediate size class of ChAT-stained MNs (Supplemental Fig. 1), precluding αMN shrinkage. Taken together, these results show that *En1-Het* mice present a loss of large αMNs in the ventral spinal cord that is first apparent at 4.5 months and progresses with time, reaching about 50% loss compared to WT at 15.5 months of age.

Recombinant hEN1 reverses the *En1-Het* motor phenotype, restores NMJ morphology and reduces αMN loss

Previously, we showed that exogenous HP transcription factors, including EN1, EN2 and OTX2, rescue mDA neurons and RGCs from an *in vivo* stress[12,13,23] and that this survival effect lasts for several weeks following a single HP injection[13,23]. This led us to test whether a single intrathecal hEN1 injection into the spinal cord of *En1-Het* mice could rescue any of the mutant neuromuscular phenotypes. In the *En1-Het* mice, muscle weakness and abnormal extensor reflex appear between 2 and 3 months, while αMN loss was first noted at 4.5 months, suggesting that three months of age is a reasonable window for hEN1 injection. One μg of hEN1 was injected and strong EN1 immunofluorescence was detected 24h later in the perivascular space and in neurons of lumbar and cervical spinal cord enlargements (Fig. 6a). ChAT immunofluorescence showed that many large-sized αMNs internalized hEN1. The number of hEN1-stained cells was lower in the cervical region probably due to its distance from the injection site in the lumbar spinal cord.

Three-month-old *En1-Het* and WT mice were evaluated for muscle strength and hindlimb extensor reflex and, 2 days later, *En1-Het* mice were separated into three groups (untreated, vehicle-injected or hEN1-injected). Injections were done with 5 μl of vehicle or 1 μg of hEN1 in 5 μl of vehicle. As already shown, before intrathecal injections, *En1-Het* mice compared to WT siblings had reduced forepaw grip strength, reduced time holding onto the inverted grid and had a slightly lower hindlimb reflex score (Fig. 6b). One and a half months later, untreated *En1-Het* mice and those treated with vehicle continued to do worse than WT mice in the three tests whereas the performance of hEN1-injected mice was indistinguishable from those of WT controls (Fig. 6b).

Synapse morphology and αMN death were analyzed in the 4.5-month-old mice injected at 3 months with vehicle or hEN1. The percentage of fully occupied endplates, reduced in *En1-Het* mice, returns to normal in hEN1-treated animals both at hindlimb and forelimb levels (Fig. 7a,b). At 3 months of age, *En1-Het* mice have a normal number of αMNs characterized by size

and ChAT staining, but some loss has already occurred 1.5 months later. Figure 7c illustrates that the number of αMNs (Cresyl violet-stained large cells) at the lumbar enlargement is similar at 4.5 months between WT mice and *En1-Het* littermates injected with hEN1 at month 3. In contrast hEN1 injection at the lumbar level did not preserve cervical αMNs from death (Fig. 7d). As a control, we produced a mutant of hEN1 (hEN1Q50A) in which glutamine in position 50 of the homeodomain was mutated into alanine. This mutant protein can be internalized but lacks high-affinity binding to DNA[33]. Supplemental Figure 4 illustrates that, in contrast with hEN1, hEN1Q50A injected at the lumbar level in 3-month-old *En1-Het* mice does not rescue muscular strength, hind limb extensor reflex, endplate occupancy or αMN number.

Taken together, these experiments demonstrate that a single hEN1 lumbar injection at month 3 restores muscle strength, normalizes the spinal reflex and restores a normal NMJ morphology. In addition, the treatment blocks lumbar, but not cervical αMN degeneration, for a period of at least 1.5 months. The absence of rescue by the hEN1Q50A variant strongly suggests that intact EN1 transcriptional activity is required for rescue. It is interesting to note that following hEN1 injection, while *En1-Het* mouse strength is restored in the forepaw grip strength and inverted grid tests, the survival of anterior level αMNs is not rescued. However, since these strength tests involve the anterior limbs, it is likely that injected hEN1 had positive effects on the physiological activity of the surviving cervical αMNs.

The effects of the hEN1 injected at 3 months in *En1-Het* mice were tested 1.5 month later, suggesting a single injection has long-lasting activity. To investigate if rescue could last more than 1.5 months, 1 µg of hEN1 was injected in 3-month-old *En1-Het* mice which were then assessed weekly during the first month following injection and then monthly up to six months. Before injection, 3-month-old *En1-Het* mice showed significant muscle weakness and an abnormal hindlimb reflex compared to WT mice (Fig. 8a-c, left side). One week after injection the forepaw grip strength and the extensor reflex in the *En1-Het* mice had returned to WT values. This improvement was fully maintained for 3 months, after which performances declined progressively to reach pre-injection levels. The improvement in the inverted grid test was more modest but followed a similar time-course. When compared to 9-month-old untreated *En1-Het* mice, *En1-Het* mice injected with hEN1 at 3 months and kept for 6 months did not maintain WT values but performed better in the 3 tests than untreated age-matched *En1-Het* mice. At the end of the study, muscles and spinal cord tissue were dissected and analyzed at the lumbar level. *En1-Het* mice treated with hEN1 show higher NMJ innervation at 9 months than

untreated age-matched *En1-Het* mice, although less than WT littermates (Fig. 9a, left panel). A similar partial rescue at 9 months was also observed for αMN survival (Fig.9b, left panel). These results suggest that a single injection of hEN1 has a long-lasting protective effect against the degenerative processes that occur in *En1-Het* mice.

Finally, we examined whether late administration of hEN1 would have any effect on the *En1-Het* phenotype by injecting 1µg of hEN1 or vehicle in 9-month-old *En1-Het* mice. Before injection, *En1-Het* mice manifested significant reductions in forepaw grip strength, time of holding onto the inverted grid and extensor reflex score (Fig. 8a-c, right side). Compared to WT siblings, vehicle and hEN1-injected *En1-Het* mice remained significantly impaired in the three tests, although, we noted a very limited improvement of the hEN1-treated *En1-Het* mice, two months post injection, for the forepaw grip strength and extensor reflex tests. At the end of the experiment the now 15.5-month-old mice were analyzed for NMJ occupancy and αMN survival. Injection after 9 months had no effect on either morphological criterion evaluated at the lumbar enlargement or for hindlimb muscles (Fig. 9a,b).

Genetic analysis reveals a regulation by hEN1 of the autophagy-associated p62 protein

The above results demonstrate non-cell autonomous physiological protection of αMNs by EN1. EN1 has been previously shown to protect mDA neurons from the SNpc[12]. To investigate if similar protective pathways are activated by EN1 in the two neuronal types, we re-analyzed the transcriptome of SNpc lysates from adult WT and *En1-Het* mice[13]. Differentially expressed genes (threshold $p<0.05$) were compared with a transcriptome analysis of WT MNs[25], and utilized for STRING analysis which resulted in 402 candidate genes (see Material and Methods). We then compared these candidates with known interactors of *En1* and of the 4 genes mutated in the most frequent familial forms of ALS: *Sod1*, *Fus*, *Tardbp-43* and *C9orf72*. This analysis provided a small list of 20 genes with potential physiological interest in the context of αMN physiology and survival.

Among this list of genes, *SQSTM1*/*p62* was found to interact with the 4 familial ALS genes, confirming a recent publication that *p62* variants were found in 486 patients with familial ALS[34]. This gene is involved in autophagy[35] and is therefore of high physio-pathological interest. To verify if its expression within αMNs is regulated by EN1, p62 levels were measured in large ChAT expressing neurons in the lumbar ventral domain of WT and *En1-Het* mice

injected with hEN1Q50A (inactive) or hEN1 (active). Injections were made at 3 months and analyzed at 4.5 months (Fig. 10). Compared to WT mice, *En1-Het* mice injected with the inactive form of EN1 show enhanced expression of p62. In contrast, *En1-Het* mice injected with the active transcription factor have expression levels identical to those of WT animals, suggesting that hEN1 regulates p62 activity.

DISCUSSION

This study establishes the importance of EN1 expression for αMN survival and motor strength. It also shows that a single intrathecal injection of hEN1 can rescue the *En1-Het* phenotype, and provide long-lasting protection when made in 9-month-old *En1-Het* mice before degeneration has reached a tipping point. In this study, we used the human recombinant protein, but the human and mouse proteins are 91.1% identical and were previously shown to have similar efficiency in mDA neuron survival experiments[12–14,17].

One day after injection, hEN1 is found around vascular structures, possibly in the perivascular space from which it penetrates into the parenchyma and reaches the cell interior. Indeed, it has been shown before that EN1 and EN2, similarly to many HPs[3,29] translocate across the plasma membrane to reach the cell cytoplasm through a mechanism distinct from endocytosis[36]. The examination of the ventral horns suggests a preferential accumulation in neurons, not precluding the possibility that other cells types may also capture the protein. Among the targeted neurons, the large neurons with a morphology evoking αMNs are systematically more strongly labeled than the medium- and small-sized ones. The histochemical and behavioral analyses of the *En1-Het* mice indicate that EN1 expressed in V1 interneurons is important for αMN function and survival. The deleterious effect of blocking extracellular EN1 with a specific anti-EN1/2 scFv expressed in and secreted from astrocytes suggests that EN1 expressed by the V1 interneurons is secreted and internalized by αMNs.

The observation that EN1 transfers preferentially to αMNs suggests they express EN1-binding sites. This hypothesis is in line with the non-cell autonomous functions of EN1/2 reported in the fly wing disk[30] and in the frog and chick optic tectum[9]. It is also reminiscent of OTX2, another HP that specifically accumulates in parvalbumin interneurons of the cerebral cortex[6]. Preceding internalization, OTX2 binds to glycosaminoglycans (GAGs) present at the surface of these interneurons thanks to the GAG binding domain (RKQRRERTTFTRAQL) that overlaps the first helix of the homeodomain[37]. Interestingly, similar GAG-binding domains are present upstream of the homeodomain in many HPs[2,3], including EN1 and EN2 for which this putative GAG-binding sequence is KEDKRPRTAFTAEQL. The potential role of this domain in the specific targeting of EN1 and the presence of EN1 binding sites at the αMN surface will be investigated in future studies.

In the *En1-Het* mouse, the extensor reflex score is reduced at 2 months, and muscle strength is reduced between 2 and 3 months. These behavioral deficits correspond to a decrease in fully occupied endplates first observed at 3 months, and precede αMN loss only first observed at 4.5 months. This temporal delay may reflect retrograde degeneration of αMNs starting at the terminals, whereby muscle strength is affected before cell body loss in the spinal cord. This recapitulates what occurs in *En1*-expressing mDA neurons in the same *En1-Het* mouse line; dopaminergic terminals in the striatum show signs of degeneration at 4 weeks, whereas the neurons only start dying at 6 weeks of age[11,38]. In this context, it is important to note that hEN1 injection at 3 months not only prevents lumbar αMNs death for months, but also restores normal endplate innervation and muscle strength. This suggests that the neurodegenerative process is slowed or halted at least for a considerable period of time. We are investigating whether repeated injections might extend this period.

The time course of αMN degeneration is rapid between 3 and 4.5 months and then slows down and eventually plateaus out to at least 15.5 months during which a minimum of ~40% αMN remain alive. It is thus possible that αMNs are heterogeneous in terms of their dependency on EN1, which is reminiscent of mDA neurons in the SNpc and Ventral Tegmental Area; the two populations express *En1*, but the latter are more resistant to *En1* hypomorphism[11]. It is also important to note that the amount of hEN1 reaching the cervical enlargement, although not sufficient to prevent the death of forelimb αMNs, restored muscle strength and endplate innervation. This indicates that levels of exogenous hEN1 that reaches the cervical spinal cord, although lower than in the lumbar enlargement close to the injection site, have beneficial effects on the remaining αMNs and restore strength as well as a normal NMJ innervation. It remains to be examined whether this involves sprouting of the remaining αMN terminals to occupy empty innervation sites.

Homeoproteins can act cell- and non-cell-autonomously. This raises two possible mechanisms leading to the phenotype observed in the *En1-Het* mice and in the protection by exogenous hEN1. A direct cell autonomous effect would mean that spinal V1 interneurons are dysfunctional in the *En1-Het* mouse. Since these cells are an essential component of the reciprocal inhibitory MN circuit, loss of their inhibitory input may place αMNs at risk[39]. Deficits in inhibitory interneurons in the spinal cord of motor neuron disease models have been

reported[40] and Renshaw cell pathology has been observed following αMN loss[41]. Alternatively, or in parallel, EN1 might act in a non-cell autonomous way. Such non-cell autonomous activity can be of several types. Firstly, EN1 may regulate within spinal V1 interneurons, the expression of classical trophic factors that are secreted to support αMN survival. Secondly, EN1 might be secreted and internalized by intermediate cell types, such as astrocytes or microglial cells, enhancing their αMN-directed trophic activity[42,43]. Finally, EN1 may transfer from V1 interneurons to αMNs where the protein would exert a direct protective activity as observed for OTX2 in RGCs[23].

It is noteworthy that neutralizing extracellular EN1 through the expression of anti-EN1/2 scFv reduces endplate innervation and muscle strength but does not induce αMN loss, at least 4 months following its expression. While longer survival times may show αMN loss, we cannot preclude that extracellular EN1 acts in conjunction with another factor secreted by WT interneurons and less so by *En1-Het* interneurons. Extracellular ENGRAILED co-signaling has been shown with DPP in the fly wing disk[30] and with EphrinA5 in the chick optic tectum[9]. It is possible that EN1 protects the αMNs that internalize it through one or several of the mechanisms characterized for mDA neurons of the SNpc, which are protected from oxidative stress by a single EN1 injection[13,14]. Among these mechanisms are the regulation, through local protein translation, of Complex I mitochondrial activity[12,16], DNA break repair, heterochromatin maintenance, and the repression of long interspersed nuclear element (LINE-1) expression[13,17]. The evaluation of these possible mechanisms in the spinal cord will be the object of future studies.

The *En1-Het* mouse presents phenotypes of muscle weaknesses, abnormal spinal reflex, NMJ denervation, and αMN loss, all of which are highly reminiscent of changes in ALS patients and in many ALS mouse models. This raises the question as to whether the results reported here are relevant for motor neuron diseases. To our knowledge, although they may exist in some sporadic cases, as is the case in Parkinson Disease[44], no ALS phenotype has been associated with mutations affecting EN1 expression. It is thus clear that the *En1-Het* mouse cannot be considered as an ALS mouse model. However, *En1* might interact genetically with pathways leading to ALS, and EN1 could be envisaged as a long-lasting therapeutic protein, as is the case in classical mouse and non-human primate models of Parkinson Disease[12–14] .

It is this reasoning and the comparison with Parkinson Disease that led us to perform our bioinformatic analysis. It is striking that we obtained only a small list of genes that interact with genes mutated in fALS. One of these genes, *SQSTM1/p62*, a well-known regulator of autophagy, associates with all 4 of the fALS genes included in our analysis, confirming a recent report that variants of the gene were found in 486 patients with fALS[34]. It is of note that p62 expression is increased in 4.5-month-old *En1-Het* mice injected at 3 months with an inactive form of EN1, but is normal in *En1-Het* mice injected with active EN1. This suggests a possible genetic interaction between *En1* and genes implicated in fALS. This hypothesis will be evaluated in future experiments involving mice heterozygote for *En1* and fALS genes (double heterozygotes) along with expression analysis of our candidate genes in gain- and loss-of-function paradigms.

In conclusion, this study offers a striking example of HP non-cell autonomous function in adult physiology and illustrates how the identification of this new physiological pathway can open the development of innovative therapeutic strategies.

FIGURE LEGENDS

Figure 1. *Engrailed-1* expression in the adult spinal cord

a. RNAscope triple *in situ* hybridization on lumbar spinal cord section shows the expression of *Engrailed-1* (*En1*), *Choline acetyl transferase* (*ChAT*) and *Calbindin-1* (*Calb1*) genes. *En1* is expressed in V1 interneurons, dorsal ($V1^P$) and ventral ($V1^R$) to the main motoneuron pool (MN). Ventral interneurons correspond to Renshaw cells characterized by *Calb1* expression. Scale bar: 500 µm

b. RT-qPCR of RNA extracted from the lumbar enlargement of 4.5- and 16-month-old of WT and *En1-Het* mouse littermates shows the stable expression of *En1* in the WT at both ages and its reduced expression in heterozygous mice.

Comparisons made by Unpaired T-test with equal SD (**p<0.005; ***p<0.0005)

Figure 2. Extracellular EN1 neutralization decreases muscular strength and modifies synapse morphology

a. Scheme of the AAV8-encoded construct expressed in the spinal cord, containing the glial fibrillary acidic protein (GFAP) promoter, the Immunoglobulin K (IgK) signal peptide for secretion, the anti-ENGRAILED single-chain antibody (AntiEN1-scFv), the 6 myc tags (6xMyc), the skipping P2A peptide and the enhanced Green Fluorescent Protein (EGFP).

b. scFv expression has no effect on weight gain before week 15 (top left). A significant effect on strength appears after week 1 for hind limb grip strength (top right) and week 6 for time on the grid (bottom left) and extensor reflex (bottom right).

c. Extracellular EN1 neutralization (16 weeks post-infection) decreases the percentage of fully occupied endplates (left) but does not affect the number of αMNs (right).

Comparisons made by Unpaired T-test with equal SD (*p<0.05; **p<0.005; ***p<0.0005; ****p<0.0001). n=6 for all groups.

Figure 3. *En1-Het* mice show progressive muscle weakness and abnormal spinal reflex

a. Body weights of *En1-Het* and WT littermates are identical at all time points.

b. Compared to their WT siblings, *En1-Het* mice show reduced normalized grip strength starting at 3 months of age.

c. Compared to their WT siblings, *En1-Het* mice hold less time onto the inverted grid, starting at 2 months of age.

d. Compared to their WT siblings, *En1-Het* mice show an abnormal hind limb reflex score, starting at 2 months of age.

Comparisons made by Unpaired T-test with equal SD comparing WT with *En1-Het* at each time point (*p<0.05; **p<0.005; ***p<0.0005; ****p<0.0001). n= 5 to 20.

Figure 4. *En1-Het* mice develop NMJ abnormalities

a. Confocal micrographs of representative images of lumbrical muscle NMJ stained for anti-neurofilament 165kDa and anti-synaptic vesicle glycoprotein 2A (2H3/SV2, red) and α-BTX (green). The area of the endplate (α-BTX+) was manually delimited (top panel, white profiles) and endplates where categorized as fully innervated (neurofilament overlying more than 80% of the endplate, white arrows), partially innervated (neurofilament overlying up to 80% of the endplate, yellow arrow) or denervated (no neurofilament overlying the endplate, blue arrows). Scale bar: 50 µm upper right panel, 25 µm other panels.

b) NMJs of *En1-Het* and WT mice do not differ for the number of AChR clusters.

c) NMJ endplate area is reduced in the *En1-Het* mice, only at 15.5 months of age.

d) The maturation state of the endplates reflected in the percentage of endplates with perforations is similar in the two genotypes through 9 months of age, but a difference appears at 15.5 months, with a reduction in the percentage of endplates with perforations in the *En1-Het* mouse.

e) Compared to WT siblings, *En1-Het* mice show a significant decrease in the percentage of fully occupied endplates starting at 3 months of age and this percentage declines with age.

Comparisons made by Unpaired T-test with equal SD comparing WT with *En1-Het* at each time point (*p<0.05; **p<0.005; ***p<0.0005; ****p<0.0001). n= 4 to 8.

Figure 5. Loss of large αMNs in the lumbar spinal cord of *En1-Het* mice

a. Representative light field micrographs of the right ventral horn of the lumbar enlargement of a WT and an *En1-Het* mouse at 15.5 months of age, stained with Cresyl violet; arrows point to examples of large cells (>300 μm^2 soma size). Scale bar: 100 µm.

b-e. No differences between *En1-Het* and WT mice were observed for the number of Nissl-stained cells with surfaces comprised between 100 and 199 μm^2 (**b**) or 200 and 299 μm^2 (**c**). In contrast, at the lumbar (**d**) and also cervical (**e**) levels, the number of large neurons corresponding to αMNs (Supplemental Fig.1) with soma surfaces > 300 μm^2 started to decrease in *En1-Het* mice at 4.5 months with a nearly 50% loss at 15.5 months. No age-associated changes in αMN number were observed in WT littermates.

Comparisons made by Unpaired T-test with equal SD comparing WT with *En1-Het* at each time point (*p<0.05; **p<0.005; ***p<0.0005; ****p<0.0001). n= 5 or 6.

Figure 6. Intrathecal hEN1 penetrates the spinal cord parenchyma and reverses the *En1-Het* motor phenotype

a. Representative confocal micrographs of the lumbar (left) and cervical (right) enlargements stained for ChAT (green) and EN1 (red) in a WT mouse 24 hours after intrathecal injection of 1 µg of hEN1 at the L5 level. Arrows show examples of cell-internalized hEN1. Arrowheads show examples of hEN1 in and/or around vessels. hEN1 injected at the lumbar level can reach ChAT-positive cells (arrows) in the cervical region (right). Scale bar: 100µm.

b. Compared to WT siblings and before hEN1 injection at 3 months of age, *En1-Het* mice have reduced forepaw grip strength (top), reduced ability to stay on the inverted grid (medium) and show an abnormal hind limb extensor score (bottom). Injection of hEN1 at 3 months of age restores all scores in 4.5-month-old *En1-Het* mice.

Comparisons made by one-way ANOVA followed by a post hoc Dunnett's test to WT (*p<0.05; **p<0.005; ***p<0.0005; ****p<0.0001). n= 7 to 22.

Figure 7. Effects of hEN1 intrathecal injection on NMJ innervation and αMN survival

a, b. *En1-Het* mice untreated or injected at 3 months with vehicle and analyzed at 4.5 months show a significant reduction in the number of fully innervated endplates; those injected with hEN1 have a percentage of fully occupied endplates similar to that found in WT mice both for lumbrical (**a**) and digitorium (**b**) muscles.

c, d. *En1-Het* mice untreated or injected at 3 months with vehicle and analyzed at 4.5 months show a significant loss of large neurons (>300 μm^2) stained with Cresyl violet while those treated with hEN1 show a complete protection against loss in the lumbar (**c**) but not in the cervical (**d**) enlargement.

Comparisons made by one-way ANOVA followed by a post hoc Dunnett's test for comparisons to WT (*p<0.05; **p<0.005; ***p<0.0005; ****p<0.0001). n= 7 to 21.

Figure 8. A single dose of hEN1 injected at 3 months, but not at 9 months, has long-lasting protective effects on *En1-Het* mice

a. *Left panel*: Reduced weight-normalized grip strength observed in *En1-Het* mice returns to control levels within one week after hEN1 injection at 3 months. This improvement lasts for 3 months before grip strength goes down again. Grip strength remains higher in injected than in non-injected mice (open square) even at 9 months. *Right panel*: 9-month-old hEN1-treated *En1-Het* mice show no recovery.

b. *Left panel*: Recovery in the inverted grid test starts at 3 weeks (no significant difference with WT siblings), lasts for 3 months and declines again thereafter. Strength remains higher in injected than in non-injected mice (open square) even at 9 months. *Right panel*: 9-month-old hEN1-treated *En1-Het* mice show no recovery.

c. *Left panel*: Recovery of the extensor reflex starts at 2 weeks, lasts for 2 months and declines again thereafter. Strength remains higher in injected than in non-injected mice (open square) even at 9 months. *Right panel*: 9-month-old hEN1-treated *En1-Het* mice show no recovery.

Comparisons made by Unpaired T-test with equal SD at each time point (*p<0.05; **p<0.005; ***p<0.0005; ****p<0.0001). n=4 to 9.

Figure 9. Injection of hEN1 at 3 months, but not at 9, reduces NMJ deterioration and αMN death

a. *Left panel*: In 9-month-old *En1-Het* mice the percentage of fully occupied endplates was significantly reduced compared to WT mice and hEN1 injection at 3 months allowed for partial recovery. *Right panel*: hEN1 injection in 9-month-old mice did not allow for recovery after 6 months.

b. *Left panel*: In 9-month-old *En1-Het* mice the number of αMN was significantly reduced compared to WT mice and hEN1 injection at 3 months allowed for partial recovery. *Right panel*: hEN1 injection in 9-month-old mice did not allow for recovery after 6 months.

Comparisons made by Unpaired T-test with equal SD (*p<0.05; **p<0.005; ***p<0.0005; ****p<0.0001). n=4 to 6.

Figure 10. The autophagy marker p62 is regulated by EN1 in αMNs

a. Double-immunostaining with an anti-SQTSM1/p62 (red) and anti-ChAT (green) antibody shows the expression of SQTSM1/p62 in αMNs from 4.5-month-old *En1-Het* mice. Scale bar: 50 µm.

b left. The quantification of anti-SQTSM1/p62 staining intensity in large ChAT-positive neurons (αMNs) demonstrates that SQTSM1/p62 expression is in increased at 4.5 months in *En1-Het* mice injected at 3 months with hEN1Q50A and returns to normal in 4.5-month-old *En1-Het* mice injected with hEN1.

Comparisons made by one-way ANOVA (****p<0.0001) n=341 to 528

b right. The distribution of SQTSM1/p62 staining intensity in large αMNs shows that the shift of the peak of intensity in *En1-Het* mice injected with hEN1Q50A is normalized in *En1-Het* mice injected with hEN1

Comparisons made by Kolmogorov–Smirnov test (*p<0.05; ****p<0.0001)

Supplemental Figure 1. Identification of αMNs by ChAT staining

a. Representative confocal micrograph (left, ChAT staining) and light field micrograph (right, Cresyl violet) of the left ventral lumbar enlargement of 9-month-old WT mouse showing manually delimited areas (white profiles). Arrows show examples of cells with somas larger than 300 μm^2. Scale bar: 100 µm.

b. The number of ChAT+ cells between 200 and 299 μm^2 (putative γMNs) is similar between genotypes (left) whereas that of cells with a surface > 300 μm^2 (αMNs) is reduced in *En1-Het* mice. Cresyl violet and ChAT staining give similar results.

Comparisons made by Unpaired T-test with equal SD (*p<0.05; **p<0.005; ***p<0.0005; ****p<0.0001). n=5 for all groups.

Supplemental Figure 2. *Engrailed-1* expression in adult midbrain nuclei and spinal cord

a. RNAscope *in situ* hybridization in the adult brain shows strong and selective expression of *Engrailed-1* in the ventral tegmental area (VTA) and Substancia Nigra (SN) of the ventral midbrain.

b. RNAscope triple *in situ* hybridization on lumbar spinal cord section shows the expression of *Engrailed-1* (red), *Choline acetyl transferase* (green) and *Calbindin-1* (blue) genes in WT (left) and *En1* heterozygote (right). Note the reduced *Engrailed-1* expression is the *En1* heterozygote.

Scale bar: 500 µm

Supplemental Figure 3. Analysis of EOM and tongue NMJs

a. In the NMJs of the EOM, the number of AChR clusters (top left), the size of endplate area (top right), the percentage of endplates with perforation (bottom left) and that of fully occupied endplates (bottom right) did not differ between *En1-Het* and WT mice.

b. In the tongue NMJs, the number of AChR clusters (top left), the size of endplate area (top right), the percentage of endplates with perforation (bottom left) and that of fully occupied endplates (bottom right) did not differ between *En1-Het* and WT mice.

Comparisons made by Unpaired T-test with equal SD comparing WT with *En1-Het* at each time point (*p<0.05; **p<0.005; ***p<0.0005; ****p<0.0001). n= 4 to 8.

Supplemental Figure 4. The hEN1Q50A mutant with reduced high affinity DNA binding does not reverse the *En1-Het* mouse phenotype

a. Scheme of the Q50A mutation in the Engrailed homeodomain

b-**e**. Compared to hEN1, hEN1Q50A has no rescuing activity in the anterior grip strength (**b**), time on the grid (**c**) and extensor reflex (**d**) tests. Accordingly, injection of the mutated protein does not protect against the decrease in endplate occupancy (**e**) or the loss of αMNs (**f**). Comparisons made by Unpaired T-test with equal SD (*$p<0.05$; **$p<0.005$; ***$p<0.0005$; ****$p<0.0001$). n=3 to 5.

References

1. Gehring, W. Homeo boxes in the study of development. *Science* **236**, 1245–1252 (1987).

2. Prochiantz, A. & Di Nardo, A. A. D. Homeoprotein signaling in the developing and adult nervous system. *Neuron* **85**, 911–925 (2015).

3. Di Nardo, A. A. D., Fuchs, J., Joshi, R. L., Moya, K. L. & Prochiantz, A. The Physiology of Homeoprotein Transduction. *Physiol Rev* **98**, 1943–1982 (2018).

4. Maizel, A., Bensaude, O., Prochiantz, A. & Joliot, A. A short region of its homeodomain is necessary for engrailed nuclear export and secretion. *Dev Camb Engl* **126**, 3183–90 (1999).

5. Derossi, D., Chassaing, G. & Prochiantz, A. Trojan peptides: the penetratin system for intracellular delivery. *Trends Cell Biol* **8**, 84–87 (1998).

6. Sugiyama, S. *et al.* Experience-dependent transfer of Otx2 homeoprotein into the visual cortex activates postnatal plasticity. *Cell* **134**, 508–520 (2008).

7. Bernard, C. *et al.* A Mouse Model for Conditional Secretion of Specific Single-Chain Antibodies Provides Genetic Evidence for Regulation of Cortical Plasticity by a Non-cell Autonomous Homeoprotein Transcription Factor. *PLOS Genetics* **12**, e1006035 (2016).

8. Kaddour, H. *et al.* Extracellular Pax6 Regulates Tangential Cajal–Retzius Cell Migration in the Developing Mouse Neocortex. *Cereb Cortex* (2019) doi:10.1093/cercor/bhz098.

9. Wizenmann, A. *et al.* Extracellular Engrailed participates in the topographic guidance of retinal axons in vivo. *Neuron* **64**, 355–366 (2009).

10. Kim, N. *et al.* Regulation of retinal axon growth by secreted Vax1 homeodomain protein. *eLife* **3**, e02671 (2014).

11. Sonnier, L. *et al.* Progressive Loss of Dopaminergic Neurons in the Ventral Midbrain of Adult Mice Heterozygote for Engrailed1. *J Neurosci* **27**, 1063–1071 (2007).

12. Alvarez-Fischer, D. *et al.* Engrailed protects mouse midbrain dopaminergic neurons against mitochondrial complex I insults. *Nature Neuroscience* **14**, 1260–1266 (2011).

13. Rekaik, H. *et al.* Engrailed Homeoprotein Protects Mesencephalic Dopaminergic Neurons from Oxidative Stress. *CellReports* **13**, 242–250 (2015).

14. Thomasson, N. *et al.* Engrailed-1 induces long-lasting behavior benefit in an experimental Parkinson primate model. *Movement Disorders* **34**, 1082–1084 (2019).

15. Brunet, I. *et al.* The transcription factor Engrailed-2 guides retinal axons. *Nature* **438**, 94–98 (2005).

16. Stettler, O. *et al.* Engrailed homeoprotein recruits the adenosine A1 receptor to potentiate ephrin A5 function in retinal growth cones. *Development* **139**, 215–224 (2012).

17. de Thé, F. B. de *et al.* Engrailed homeoprotein blocks degeneration in adult dopaminergic neurons through LINE-1 repression. *Embo J* **37**, (2018).

18. Sapir, T. Pax6 and Engrailed 1 Regulate Two Distinct Aspects of Renshaw Cell Development. *Journal of Neuroscience* **24**, 1255–1264 (2004).

19. Benito-Gonzalez, A. & Alvarez, F. J. Renshaw cells and Ia inhibitory interneurons are generated at different times from p1 progenitors and differentiate shortly after exiting the cell cycle. *The Journal of neuroscience : the official journal of the Society for Neuroscience* **32**, 1156–1170 (2012).

20. Ramírez-Jarquín, U. N., Lazo-Gómez, R., Tovar-y-Romo, L. B. & Tapia, R. Spinal inhibitory circuits and their role in motor neuron degeneration. *Neuropharmacology* **82**, 101–107 (2014).

21. Hanks, M., Wurst, W., Anson-Cartwright, L., Auerbach, A. & Joyner, A. Rescue of the En-1 mutant phenotype by replacement of En-1 with En-2. *Science* **269**, 679–682 (1995).

22. Sleigh, J. N., Burgess, R. W., Gillingwater, T. H. & Cader, M. Z. Morphological analysis of neuromuscular junction development and degeneration in rodent lumbrical muscles. *J Neurosci Meth* **227**, 159–165 (2014).

23. Torereo -Ibad, R. T. *et al.* Otx2 promotes the survival of damaged adult retinal ganglion cells and protects against excitotoxic loss of visual acuity in vivo. *The Journal of neuroscience : the official journal of the Society for Neuroscience* **31**, 5495–5503 (2011).

24. Hylden, J. L. K. & Wilcox, G. L. Intrathecal morphine in mice: A new technique. *Eur J Pharmacol* **67**, 313–316 (1980).

25. Bandyopadhyay, U. *et al.* RNA-Seq Profiling of Spinal Cord Motor Neurons from a Presymptomatic SOD1 ALS Mouse. *Plos One* **8**, e53575 (2013).

26. Comley, L. H., Nijssen, J., Frost-Nylen, J. & Hedlund, E. Cross-disease comparison of amyotrophic lateral sclerosis and spinal muscular atrophy reveals conservation of selective vulnerability but differential neuromuscular junction pathology. *Journal of Comparative Neurology* **524**, 1424–1442 (2016).

27. Bikoff, J. B. *et al.* Spinal Inhibitory Interneuron Diversity Delineates Variant Motor Microcircuits. *Cell* **165**, 207–219 (2016).

28. Di Nardo, A. A. D. *et al.* Dendritic localization and activity-dependent translation of Engrailed1 transcription factor. *Molecular and Cellular Neuroscience* **35**, 230–236 (2007).

29. Lee, E. J. *et al.* Global Analysis of Intercellular Homeodomain Protein Transfer. *Cell Reports* **28**, 712-722.e3 (2019).

30. Layalle, S. *et al.* Engrailed homeoprotein acts as a signaling molecule in the developing fly. *Development* **138**, 2315–2323 (2011).

31. Sanes, J. R. & Lichtman, J. W. Development of the vertebrate neuromuscular junction. *Annual Review of Neuroscience* **22**, 389–442 (1999).

32. Powis, R. A. & Gillingwater, T. H. Selective loss of alpha motor neurons with sparing of gamma motor neurons and spinal cord cholinergic neurons in a mouse model of spinal muscular atrophy. *Journal of Anatomy* **228**, 443–451 (2016).

33. Le Roux, I. L., Joliot, A. H., Bloch-Gallego, E., Prochiantz, A. & Volovitch, M. Neurotrophic activity of the Antennapedia homeodomain depends on its specific DNA-binding properties. *Proceedings of the National Academy of Sciences* **90**, 9120–9124 (1993).

34. Yilmaz, R. *et al.* SQSTM1/p62 variants in 486 familial ALS patients from Germany and Sweden. *Neurobiol Aging* (2019) doi:10.1016/j.neurobiolaging.2019.10.018.

35. Kumsta, C. *et al.* The autophagy receptor p62/SQST-1 promotes proteostasis and longevity in C. elegans by inducing autophagy. *Nat Commun* **10**, 5648 (2019).

36. Joliot, A. & Prochiantz, A. Transduction peptides: from technology to physiology. *Nature Cell Biology* **6**, 189–196 (2004).

37. Beurdeley, M. *et al.* Otx2 Binding to Perineuronal Nets Persistently Regulates Plasticity in the Mature Visual Cortex. *Journal of Neuroscience* **32**, 9429–9437 (2012).

38. Nordström, U. *et al.* Progressive nigrostriatal terminal dysfunction and degeneration in the engrailed1 heterozygous mouse model of Parkinson's disease. *Neurobiology of Disease* **73**, 70–82 (2015).

39. Quinlan, K. A. Links between electrophysiological and molecular pathology of amyotrophic lateral sclerosis. *Integrative and comparative biology* **51**, 913–925 (2011).

40. Hossaini, M. *et al.* Spinal Inhibitory Interneuron Pathology Follows Motor Neuron Degeneration Independent of Glial Mutant Superoxide Dismutase 1 Expression in SOD1-ALS Mice. *Journal of Neuropathology and Experimental Neurology* **70**, 662–677 (2011).

41. Chang, Q. & Martin, L. J. Glycinergic innervation of motoneurons is deficient in amyotrophic lateral sclerosis mice: a quantitative confocal analysis. *The American Journal of Pathology* **174**, 574–585 (2009).

42. Qian, K. *et al.* Sporadic ALS Astrocytes Induce Neuronal Degeneration In Vivo. *Stem Cell Reports* **8**, 843–855 (2017).

43. Barber, S. C., Mead, R. J. & Shaw, P. J. Oxidative stress in ALS: A mechanism of neurodegeneration and a therapeutic target. *Biochimica Et Biophysica Acta Bba - Mol Basis Dis* **1762**, 1051–1067 (2006).

44. Haubenberger, D. *et al.* Association of transcription factor polymorphisms PITX3 and EN1 with Parkinson's disease. *Neurobiol Aging* **32**, 302–307 (2011).

Figure 1. *Engrailed-1* expression in the adult spinal cord

a

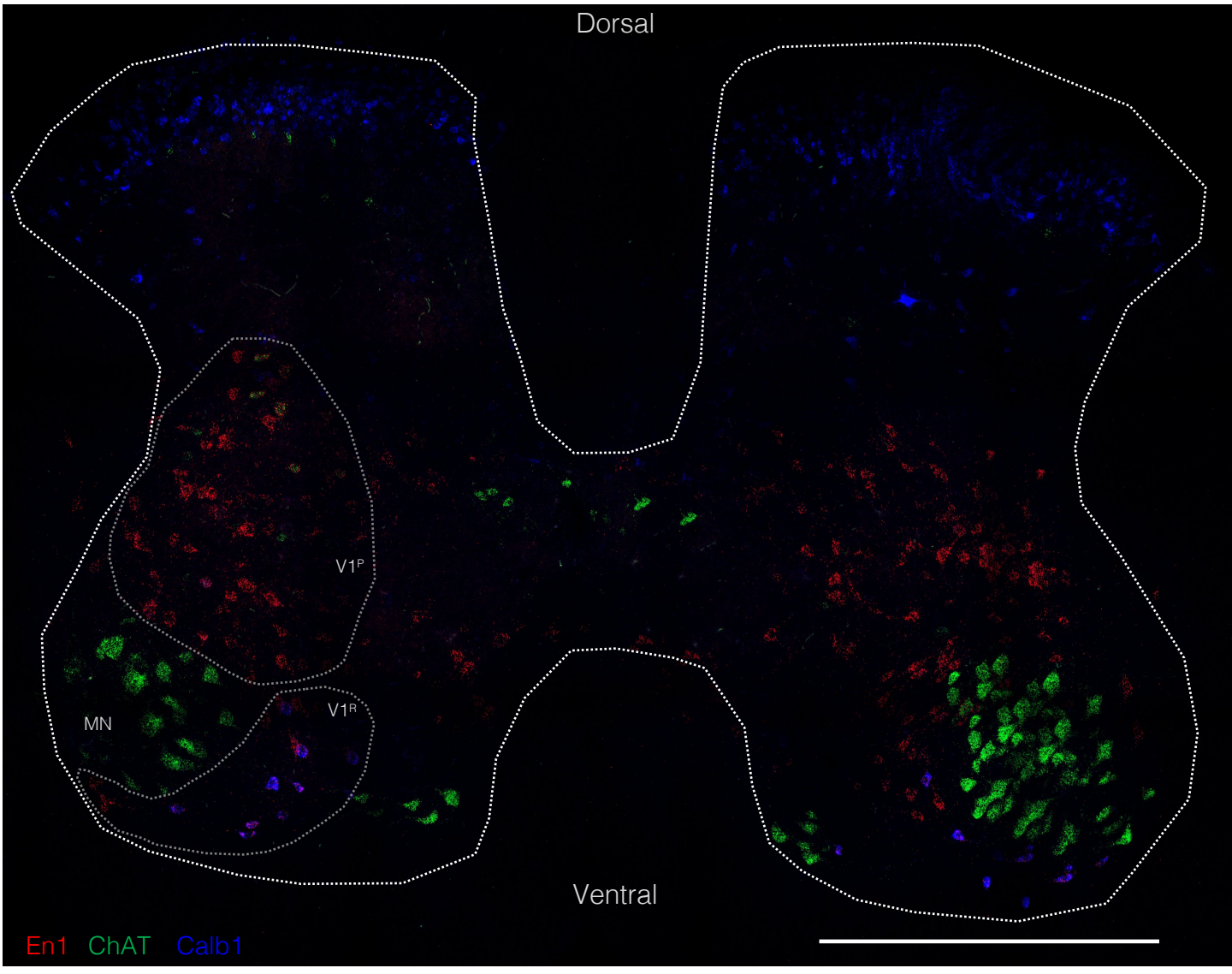

b

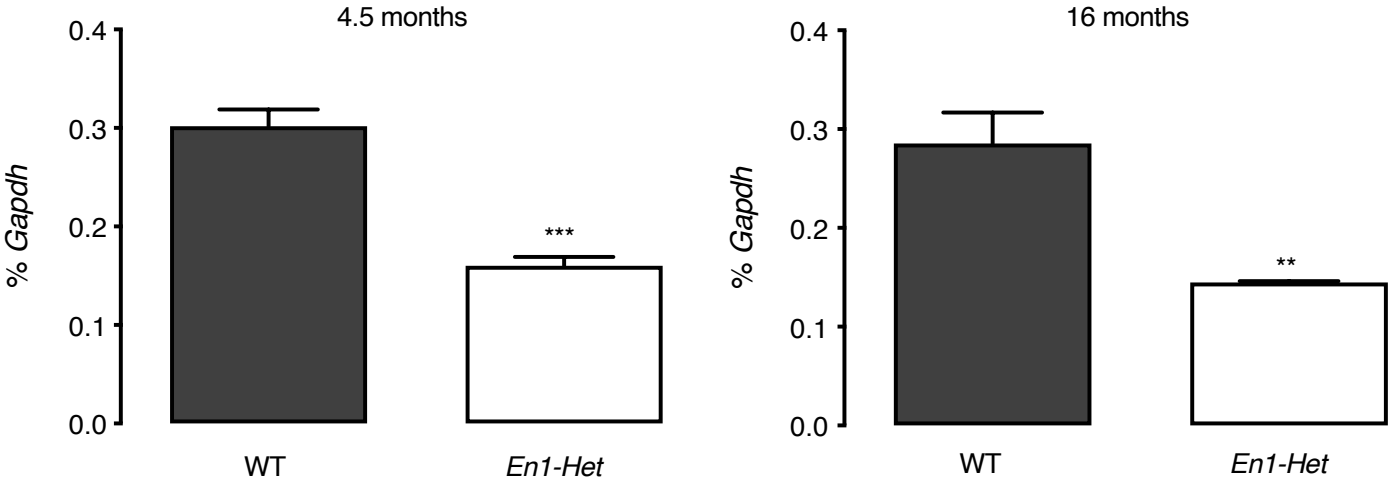

Figure 2. Extracellular EN1 neutralization decreases muscular strength and modifies synapse morphology

a

b

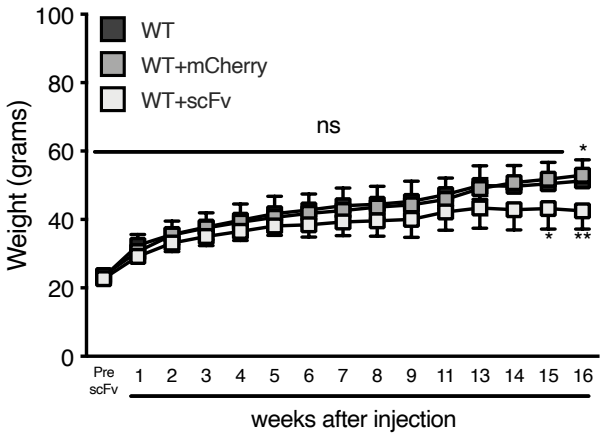

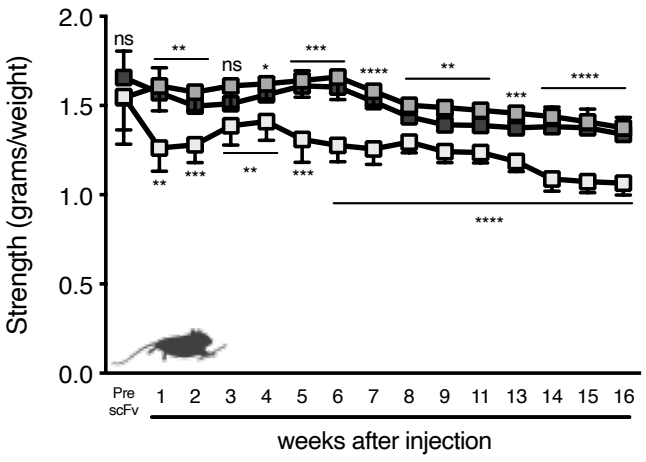

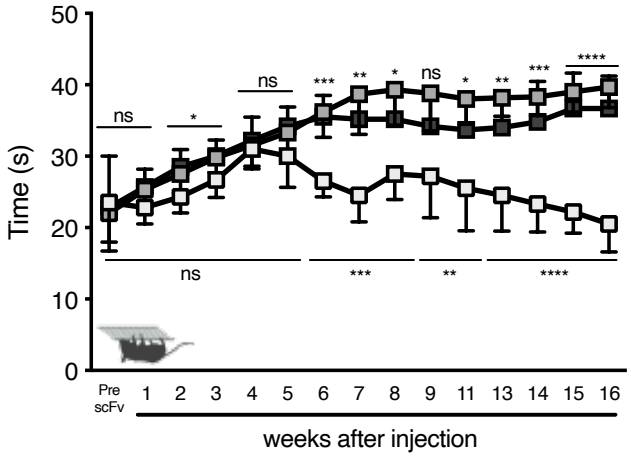

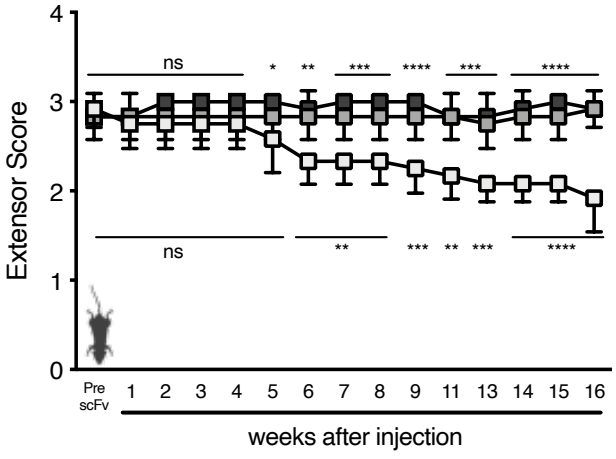

c

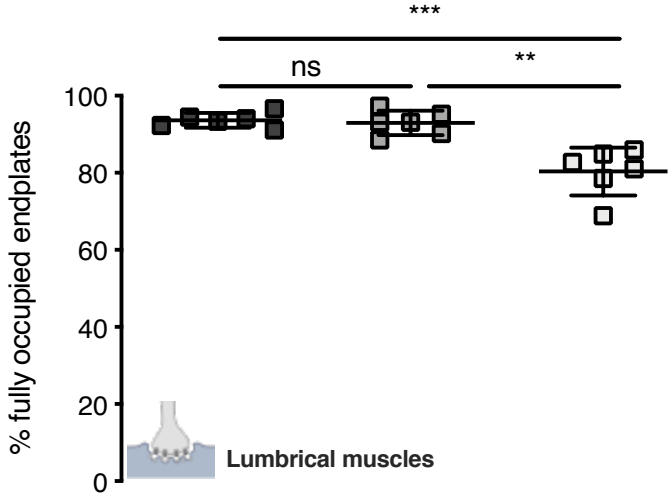

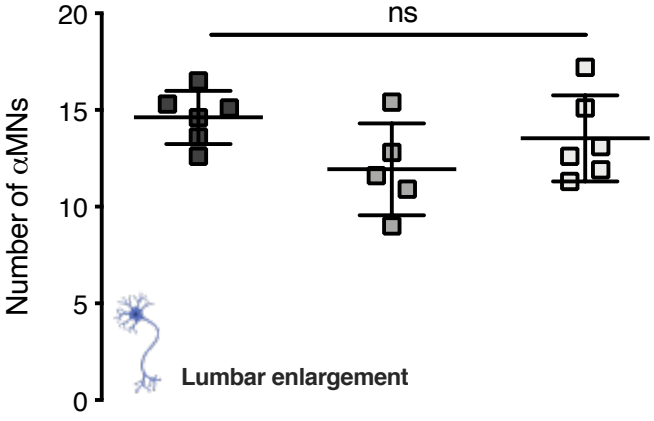

Figure 3. *En1 -Het* mice show progressive muscle weakness and abnormal spinal reflex

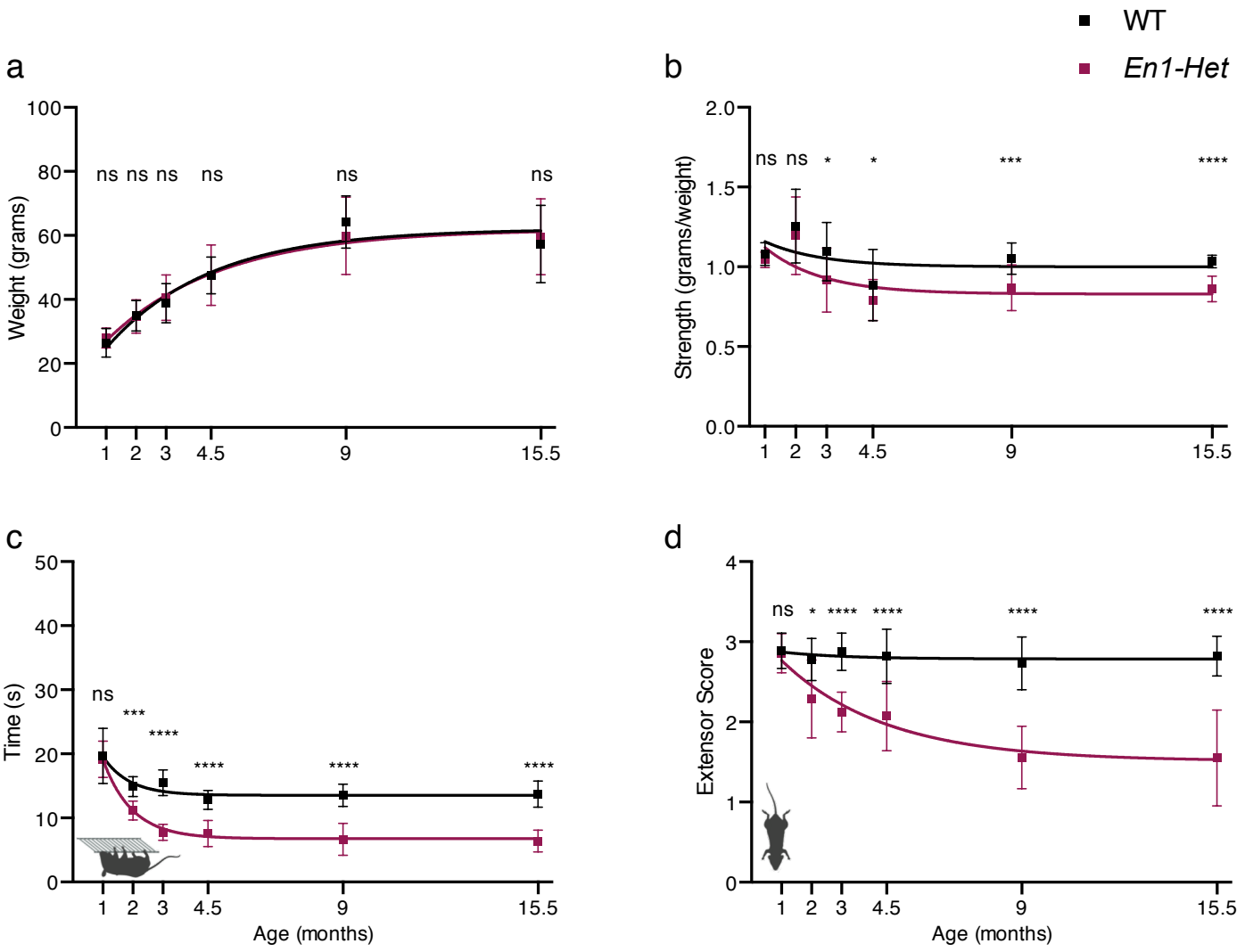

Figure 4. *En1-Het* mice develop NMJ abnormalities

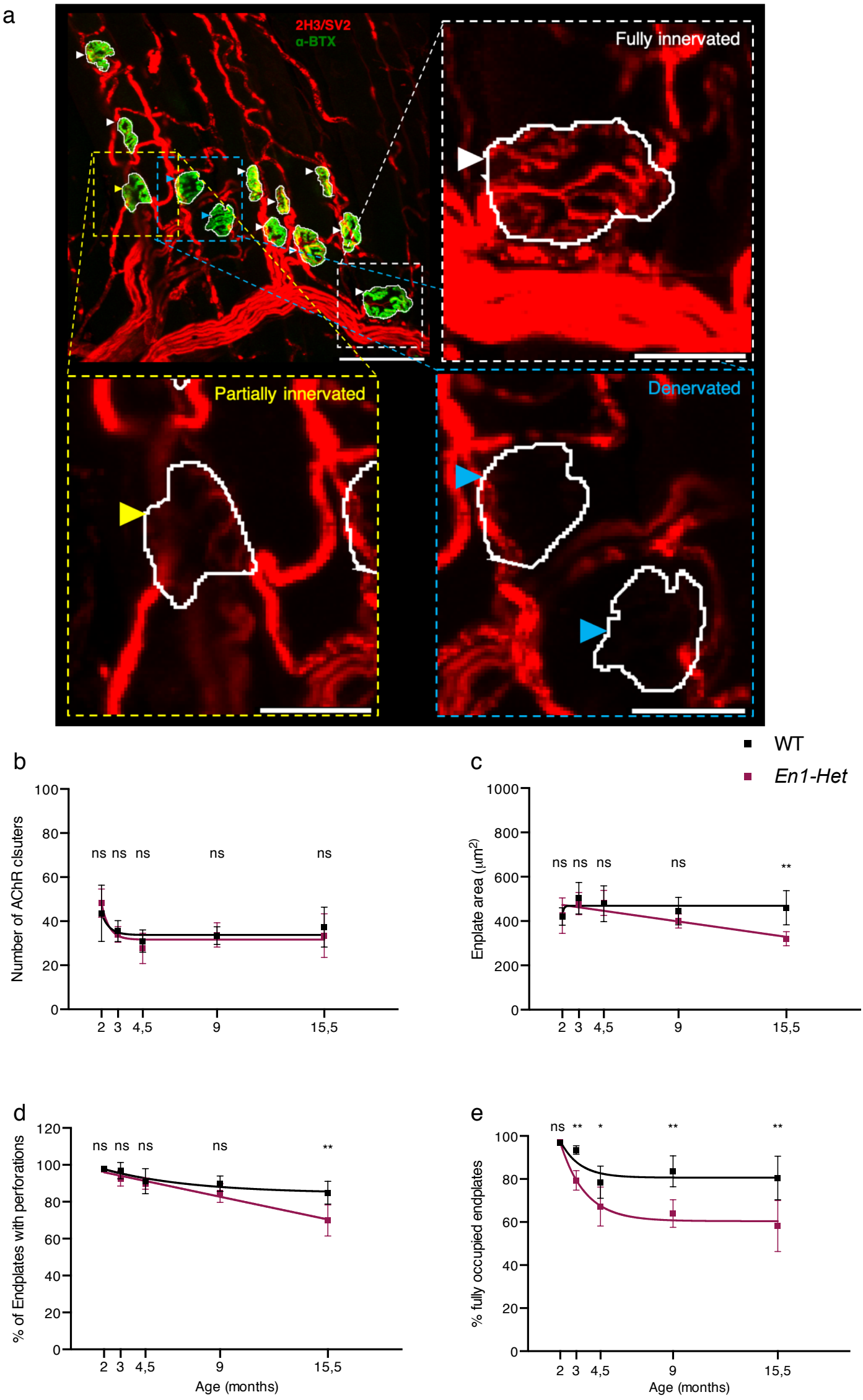

Figure 5. Loss of large αMNs in lumbar spinal cord of *En1-Het* mice

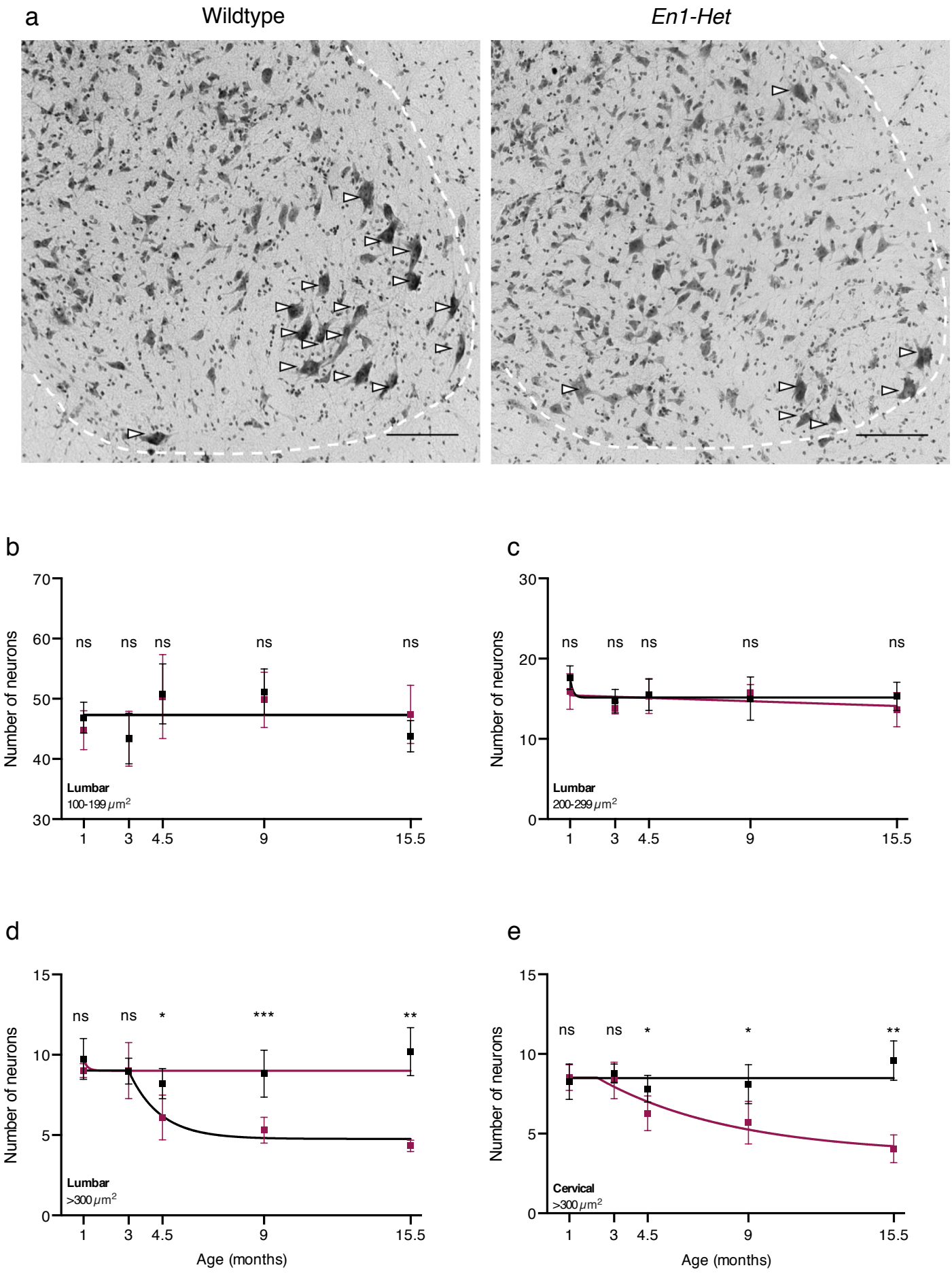

Figure 6. Intrathecal hEN1 penetrates the spinal cord parenchyma and reverses the *En1-Het* motor phenotype

a

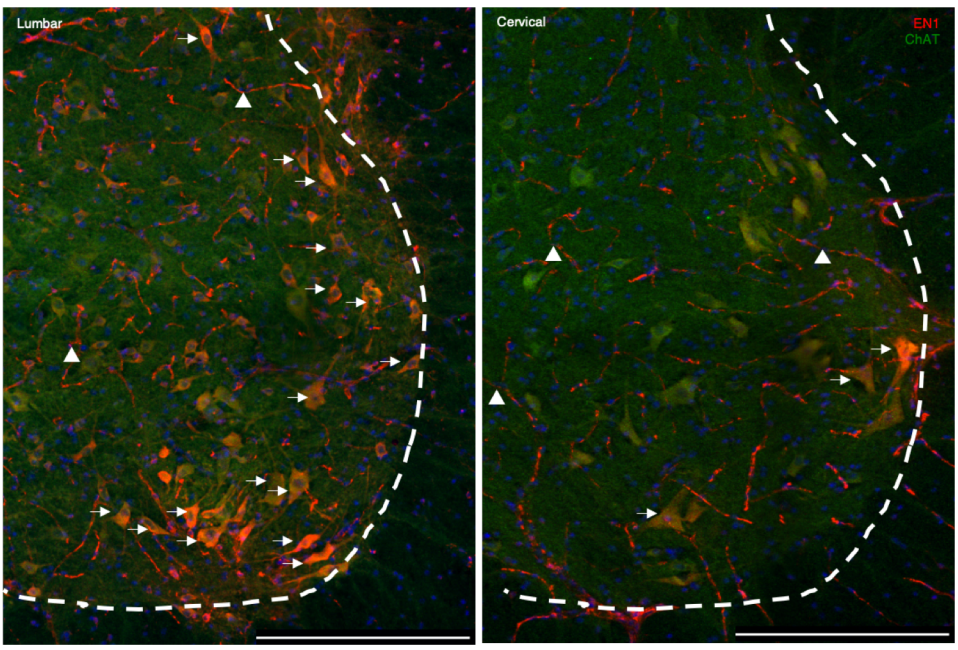

b

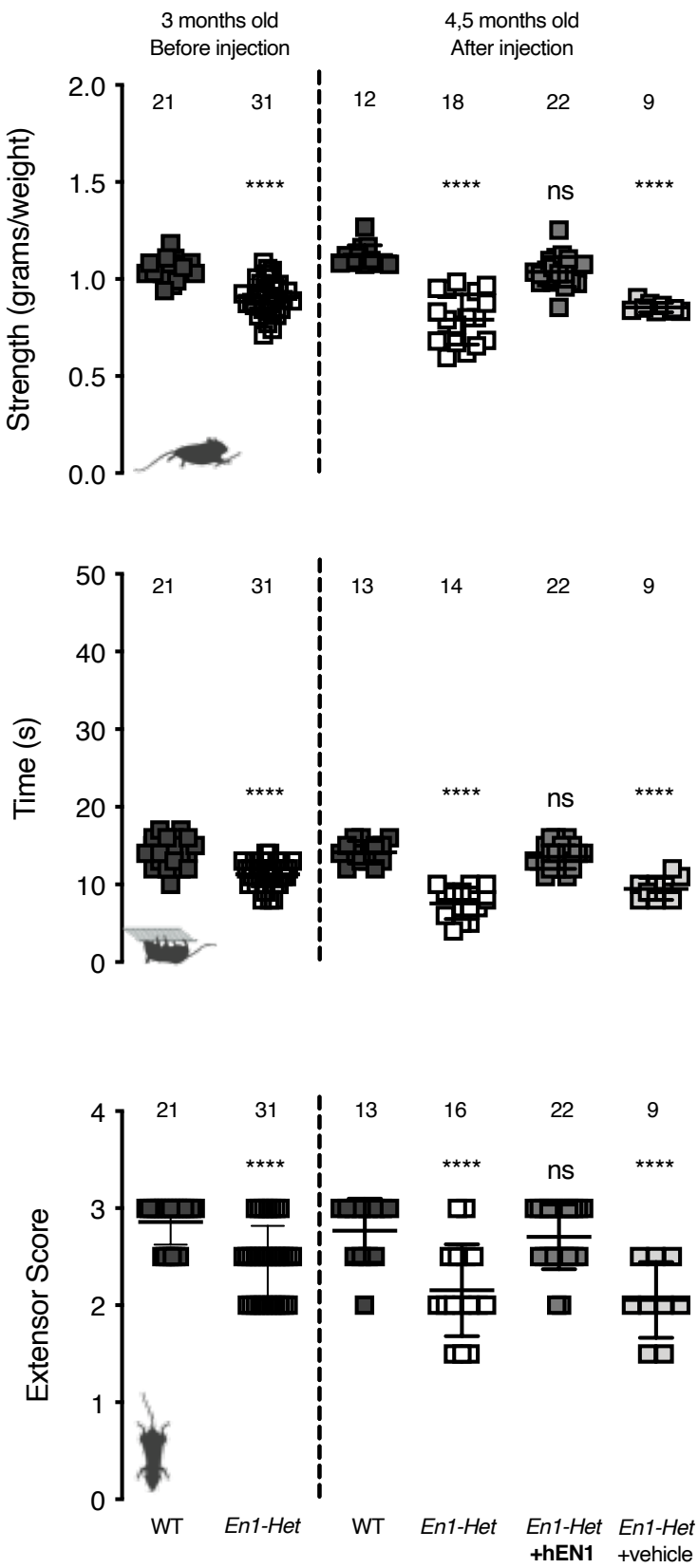

Figure 7. Effects of hEN1 intrathecal injection on NMJ innervation and αMN survival

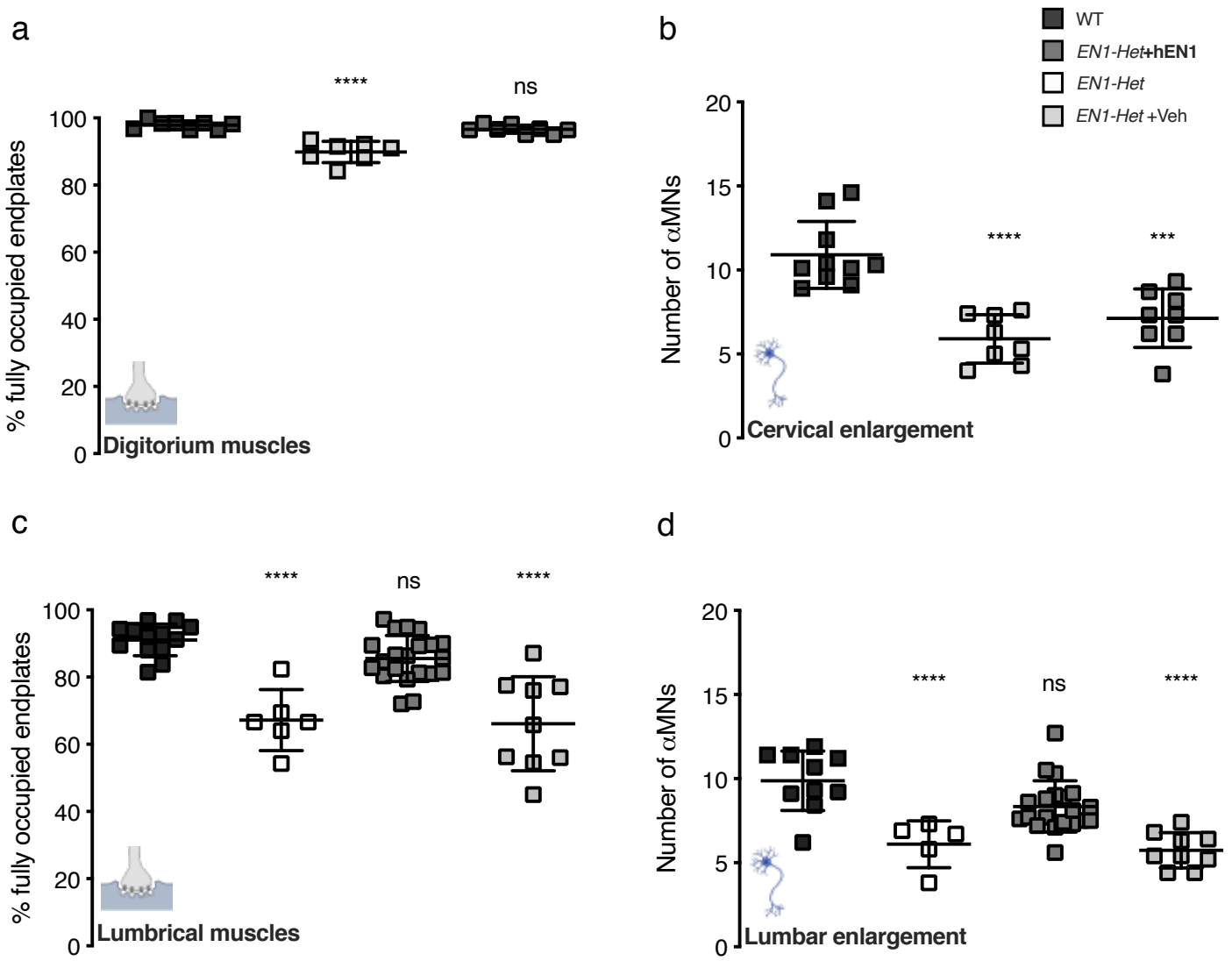

Figure 8. A single dose of hEN1 injected at 3 months, but not at 9, has long lasting protective effects on *En1-Het* mice

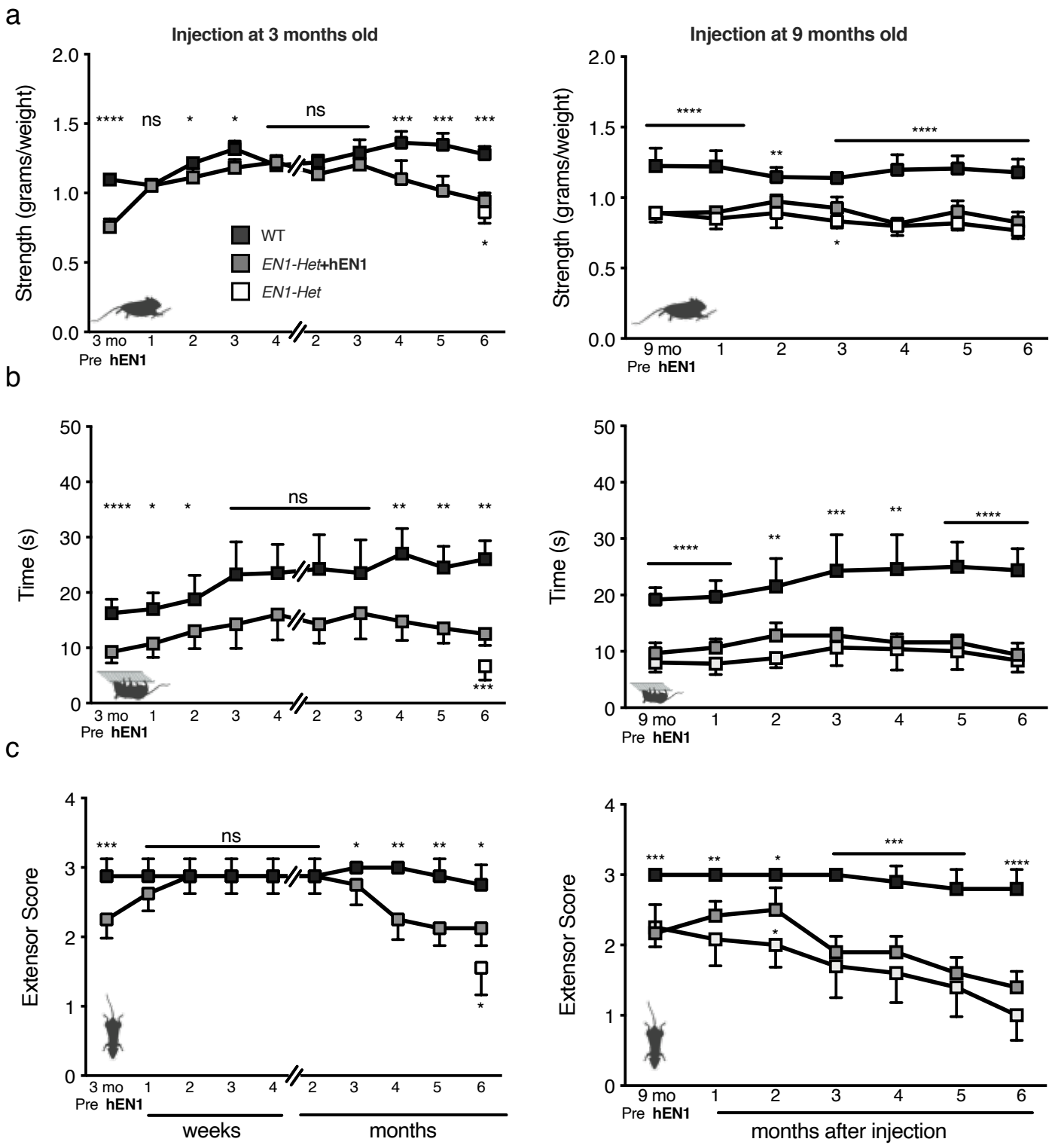

Figure 9. Injection of hEN1 at 3 months, but not at 9, reduces NMJ deterioration and αMN death

a

9 months old

15 months old

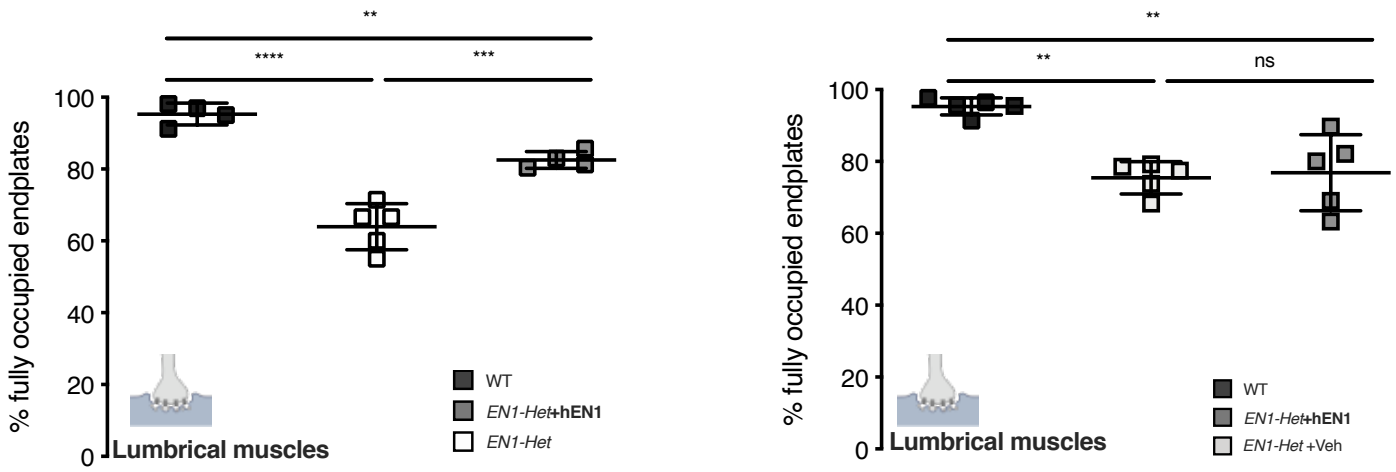

b

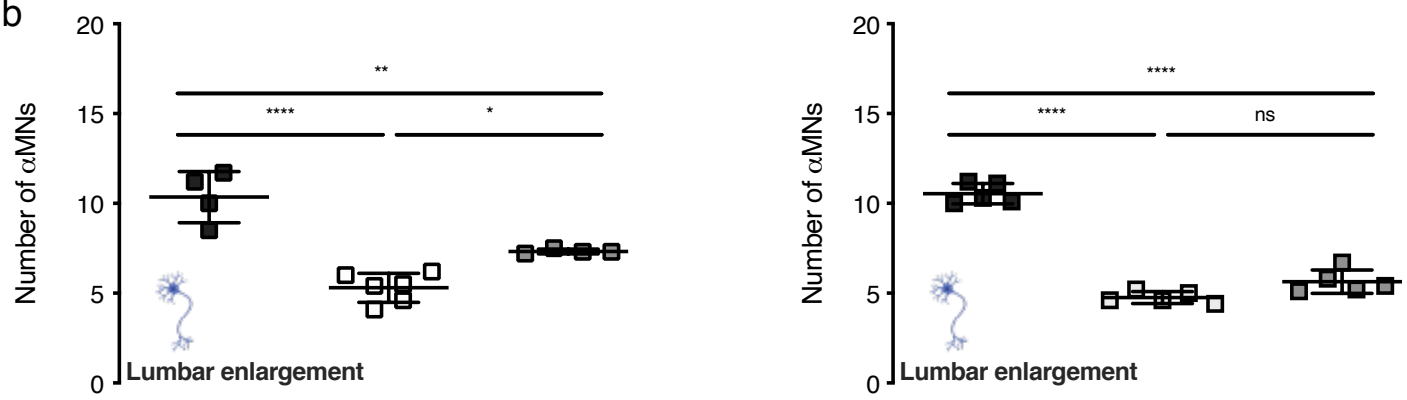

Figure 10. The autophagy maker p62 is regulated by EN1 in αMNs

a

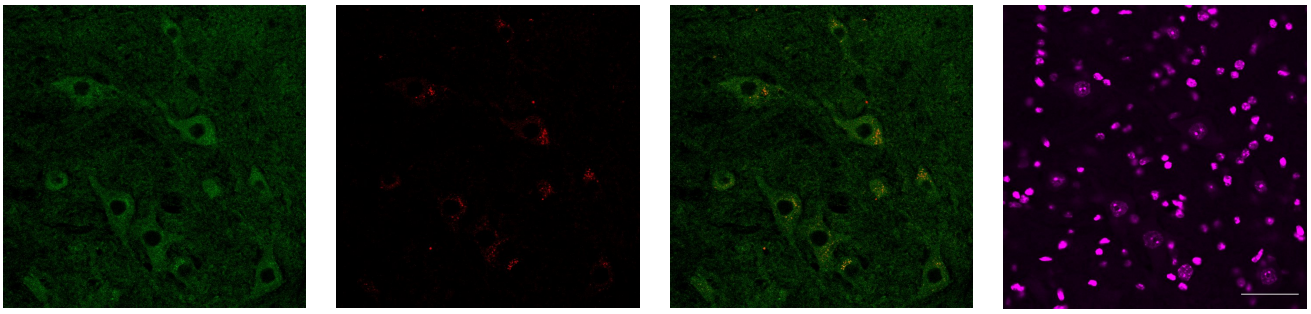

b

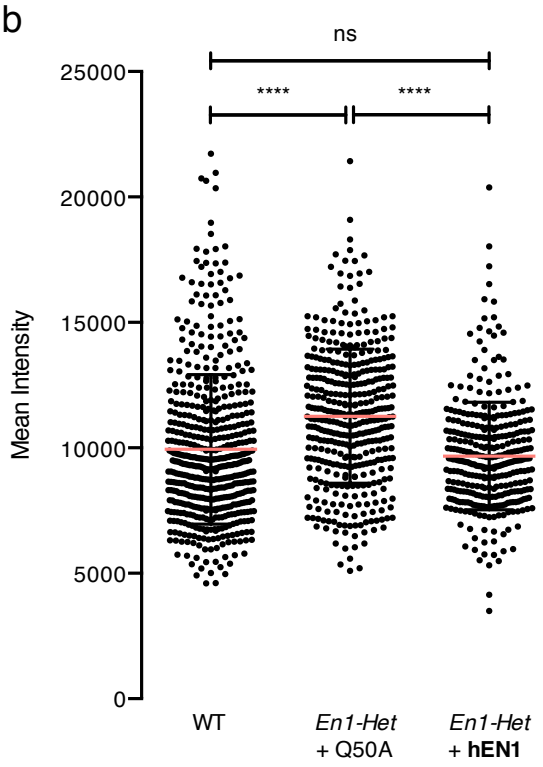

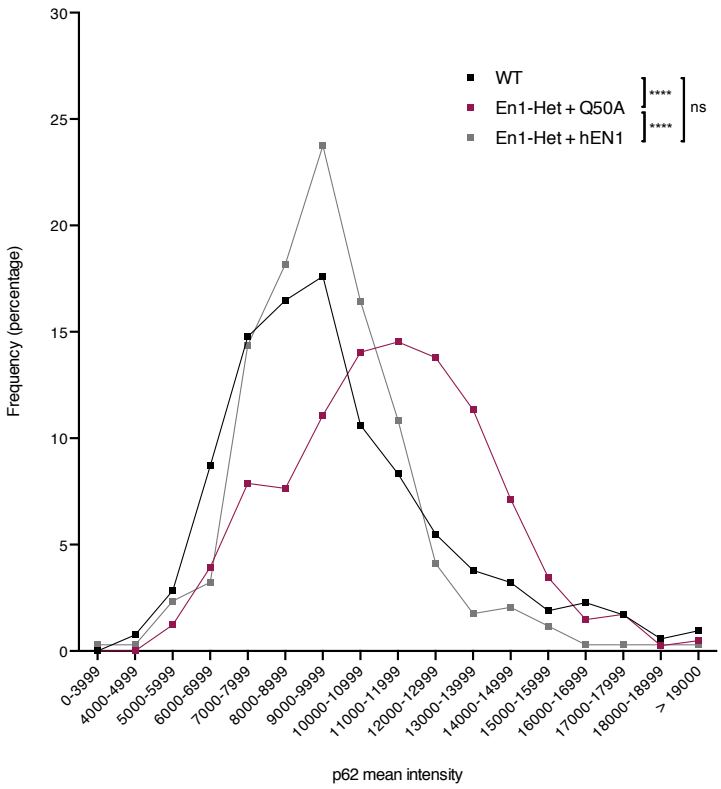

Supplemental Figure 1. Identification of αMNs by ChAT staining

a

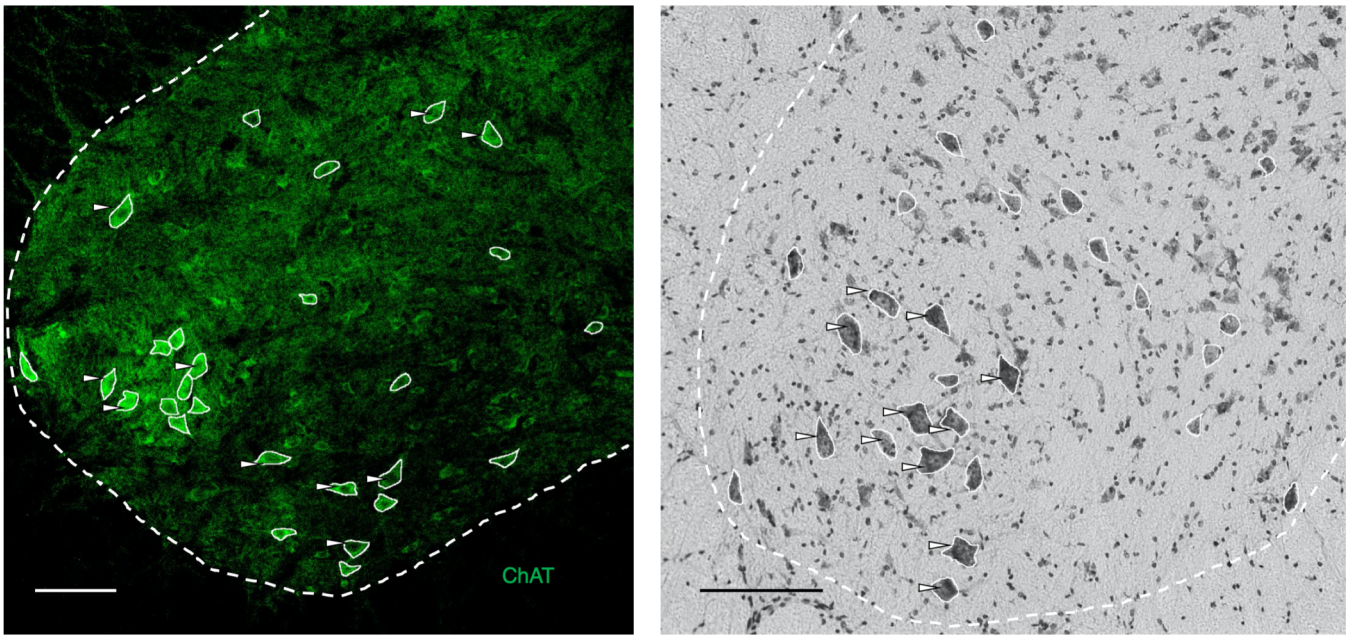

9 months old
Lumbar

b

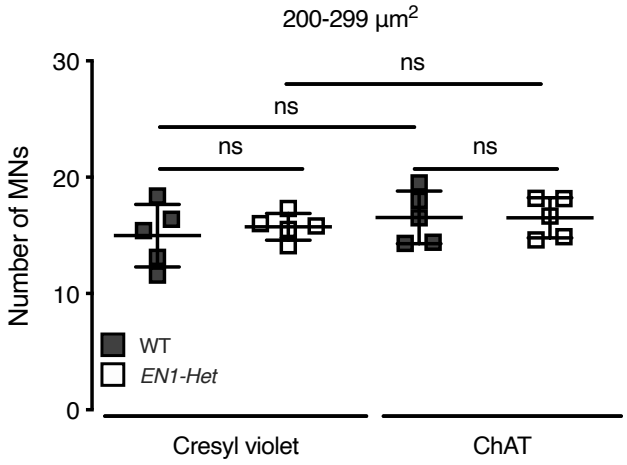

c

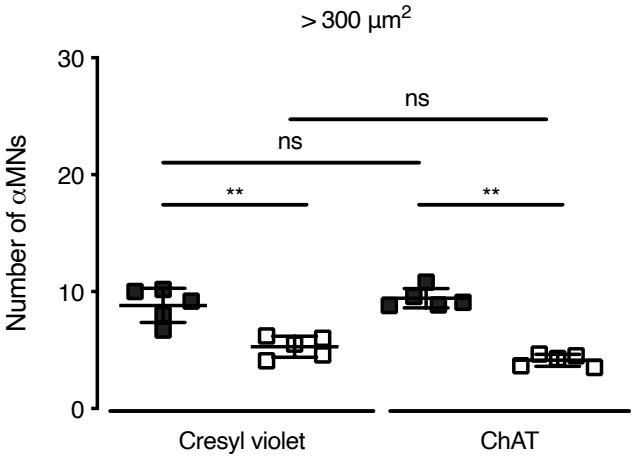

Supplemental Figure 2. *Engrailed-1* expression in adult midbrain nuclei and spinal cord

a

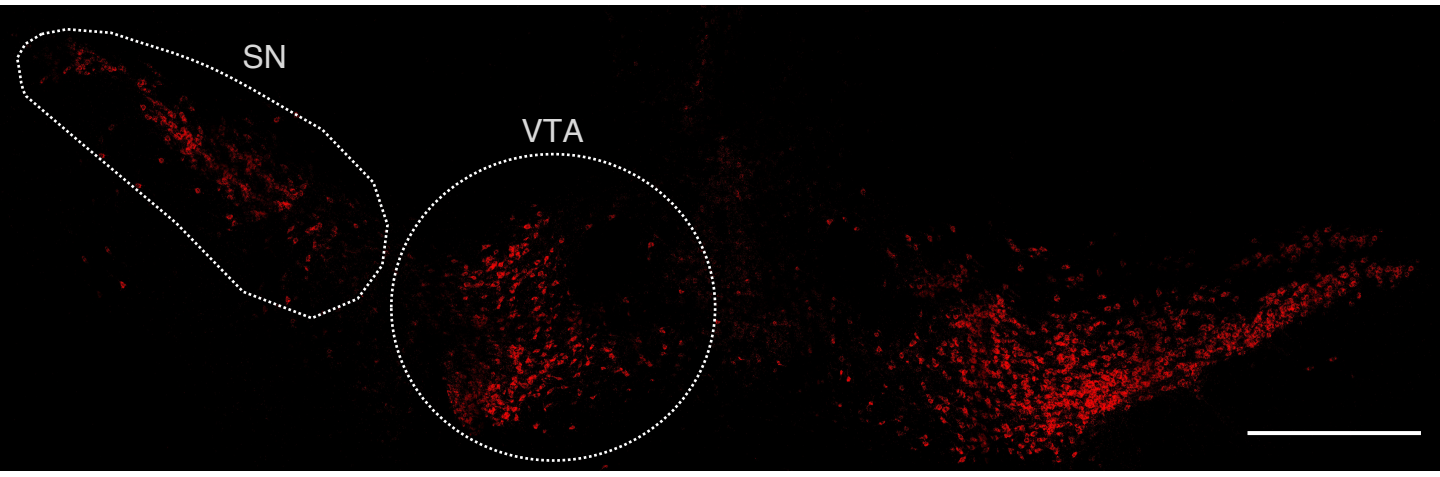

b

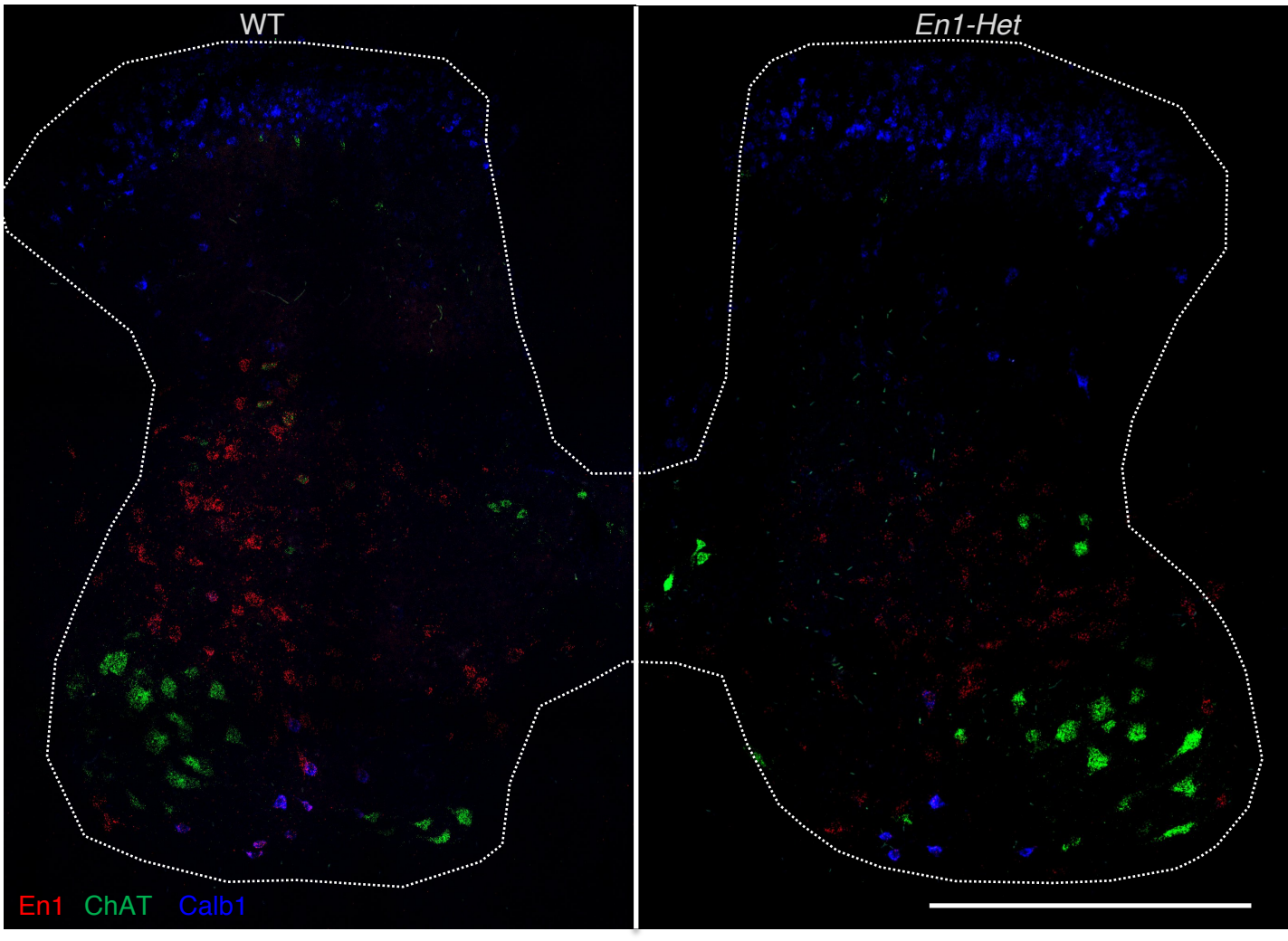

Supplemental Figure 3. Analysis of EOM and tongue NMJs

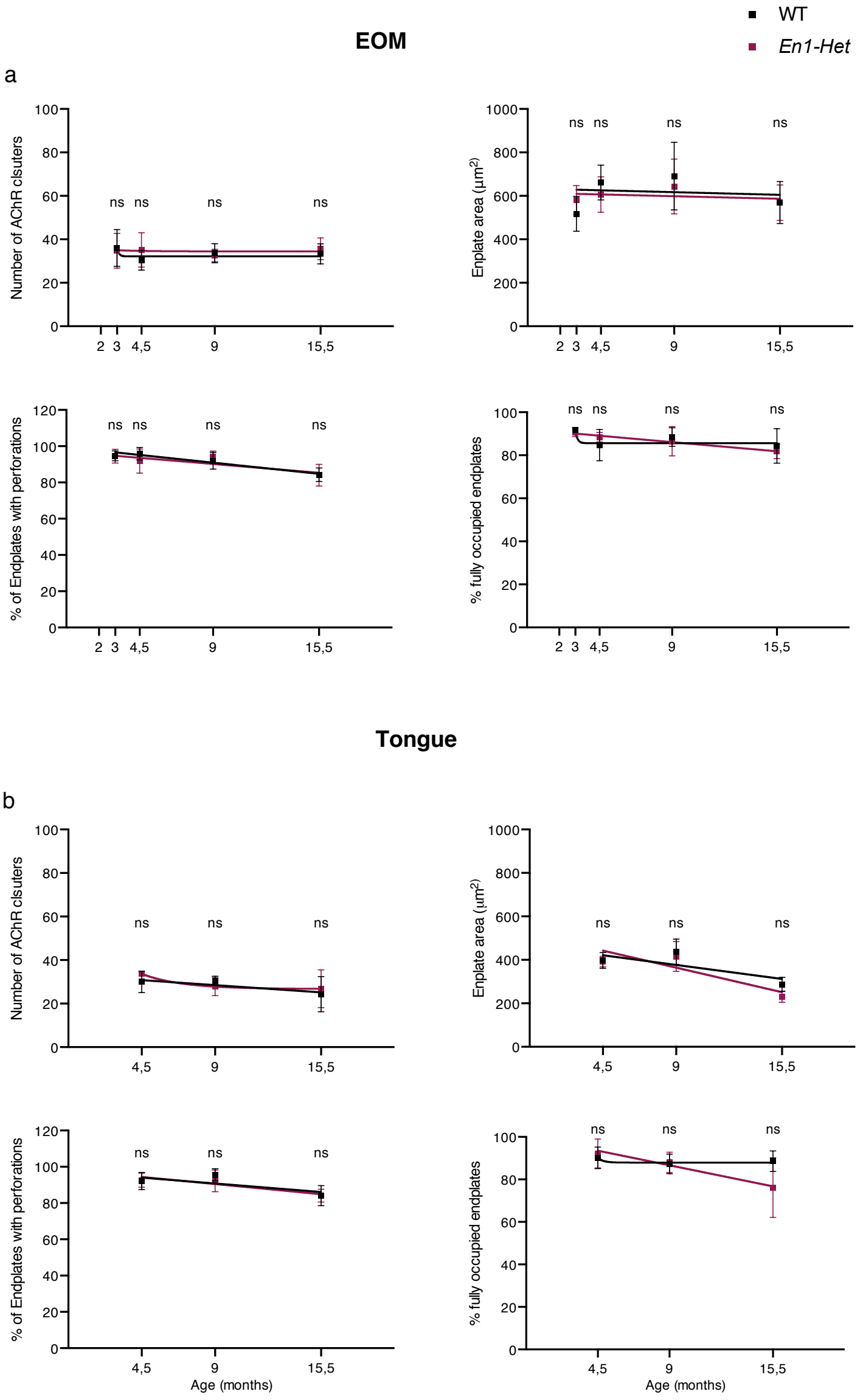
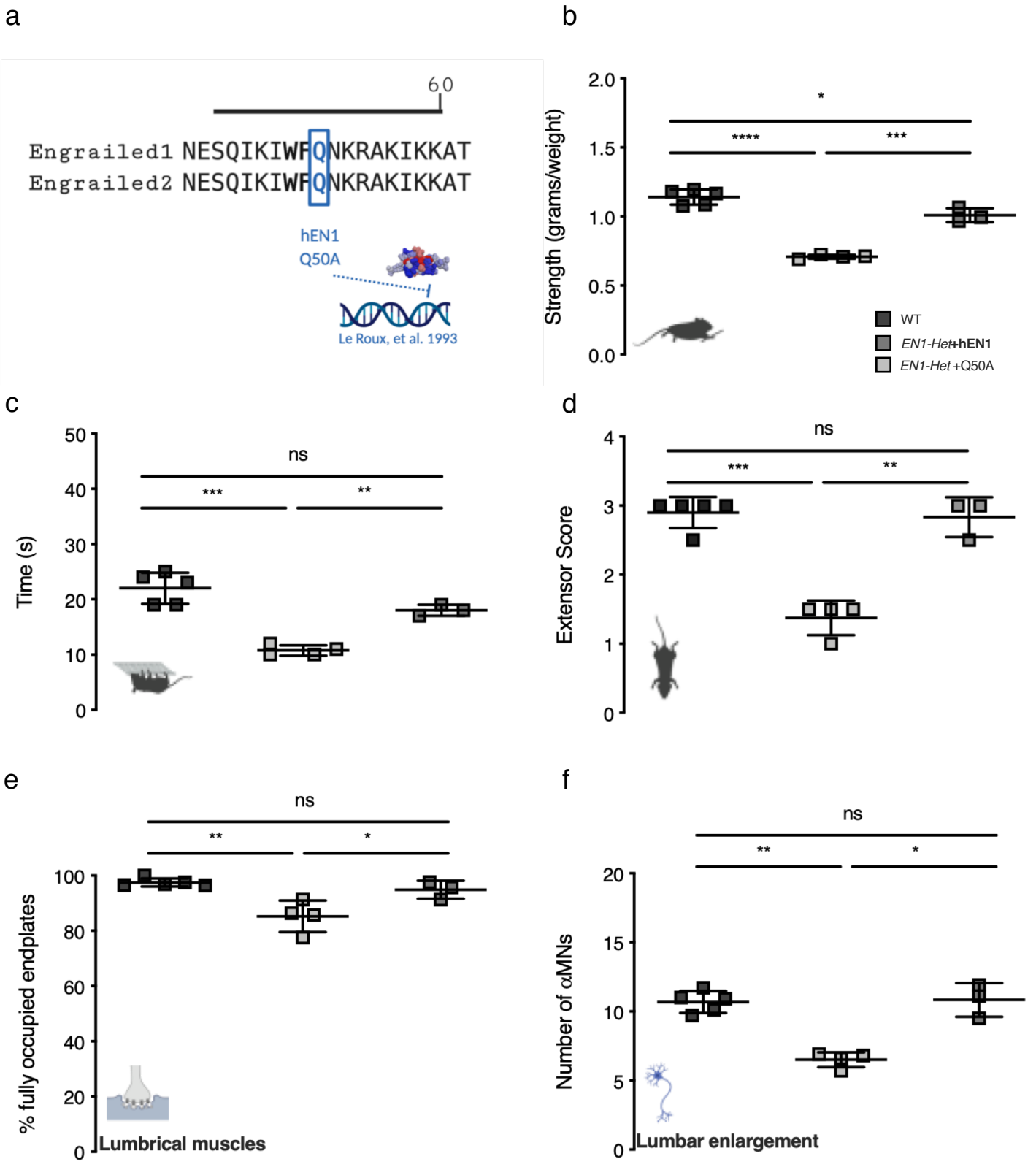
Supplemental Figure 4. The hEN1Q50A mutant with reduced high affinity DNA binding does not reverse the *En1-Het* mouse phenotype